US006721057B1

(12) **United States Patent** (10) **Patent No.:** **US 6,721,057 B1**
Reininger (45) **Date of Patent:** **Apr. 13, 2004**

(54) **SPATIALLY MODULATED INTERFEROMETER AND BEAM SHEARING DEVICE THEREFOR**

(75) Inventor: **Francis M. Reininger**, Irvine, CA (US)

(73) Assignee: **California Institute of Technology**, Pasadena, CA (US)

(*) Notice: Subject to any disclaimer, the term of this patent is extended or adjusted under 35 U.S.C. 154(b) by 0 days.

(21) Appl. No.: **09/547,790**

(22) Filed: **Apr. 12, 2000**

Related U.S. Application Data

(60) Provisional application No. 60/129,383, filed on Mar. 13, 1999.

(51) **Int. Cl.**^{7} **G01B 9/02**
(52) **U.S. Cl.** **356/520**; 356/450
(58) **Field of Search** 356/450, 520

(56) **References Cited**

U.S. PATENT DOCUMENTS

4,213,706 A	*	7/1980	Hill et al.	....	356/520
4,395,123 A	*	7/1983	Minott	....	356/510
4,509,857 A		4/1985	Vermande	....	356/346
4,523,846 A		6/1985	Breckinridge et al.	......	356/346
4,531,197 A	*	7/1985	Lin	....	359/285
4,773,732 A	*	9/1988	Schafer	....	359/578
4,976,542 A		12/1990	Smith	....	356/346
5,059,027 A		10/1991	Roesler et al.	....	356/346
5,266,795 A		11/1993	Vaughan		
5,768,040 A		6/1998	Macenka et al.	....	359/859
5,777,736 A		7/1998	Horton	....	356/346
5,781,293 A		7/1998	Padgett et al.	....	356/346
5,880,834 A		3/1999	Chrisp		
5,999,311 A	*	12/1999	Nanba et al.	....	359/365

OTHER PUBLICATIONS

Hirst et al., "Optical sensors: a path to better gas detection", Global Challenges, Physics World, Aug. 1998, pp. 37–40.
Dohi et al., "Attainment of High Resolution Holographic Fourier Transform Spectroscopy", Applied Optics, May 1971, pp 1137–1140, vol. 10, No. 5.
Stroke et al., "Fourier–Transform Spectroscopy Using Holographic Imaging Without Computing and With Stationary Interferometers", Physics Letters, Jun. 1, 1965, pp. 272–274, vol. 16, No. 3.
Barnes, "Photodiode array Fourier transform spectrometer with improved dynamic range", Applied Optics, Nov. 15, 1985, pp. 3702–3706, vol. 24, No. 22.
Okamoto et al., "Fourier transform spectrometer with a self–scanning photodiode array", Applied Optics, Jan. 15, 1984, pp. 269–273, vol. 23, No. 2.
Flamini, Enrico et al.; *Remote mineralogy through multi-spectral imaging, the VIMS–V instrument*; 10 pp.
Lobb, D.R.; *Theory of concentric designs for grating spectrometers*; Applied Optics; May 1, 1994; vol. 33, No. 13, pp. 2648–2658.

(List continued on next page.)

Primary Examiner—T. Chowdhury
Assistant Examiner—George Wang
(74) *Attorney, Agent, or Firm*—Christie, Parker & Hale, LLP

(57) **ABSTRACT**

A spatially modulated interferometer incorporates a beam shearing system having a plurality of reflective surfaces defining separate light paths of equal optical path length for two separate output beams. The reflective surfaces are arranged such that when the two beams emerge from the beam shearing system they contain more than 50 percent of the photon flux within the selected spectral pass band. In one embodiment, the reflective surfaces are located on a number of prism elements combined to form a beam shearing prism structure. The interferometer utilizing the beam sharing system of the invention includes fore-optics for collecting light and focusing it into a beam to be sheared, and a detector located at an exit pupil of the device. In a preferred embodiment, the interferometer has no moving parts.

34 Claims, 19 Drawing Sheets
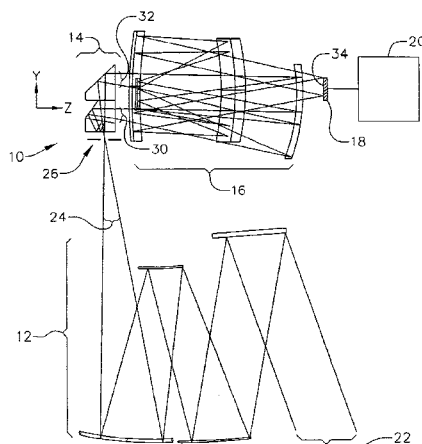
OTHER PUBLICATIONS

Mertz, L.; *Concentric spectographs*; Applied Optics; Dec. 1977; vol. 16, No. 12; pp. 3122–3124.

Offner, A.; *New Concepts in Projection Mask Aligners*; Optical Engineering; Mar.–Apr. 1975; vol. 14, No. 2; pp. 130–132.
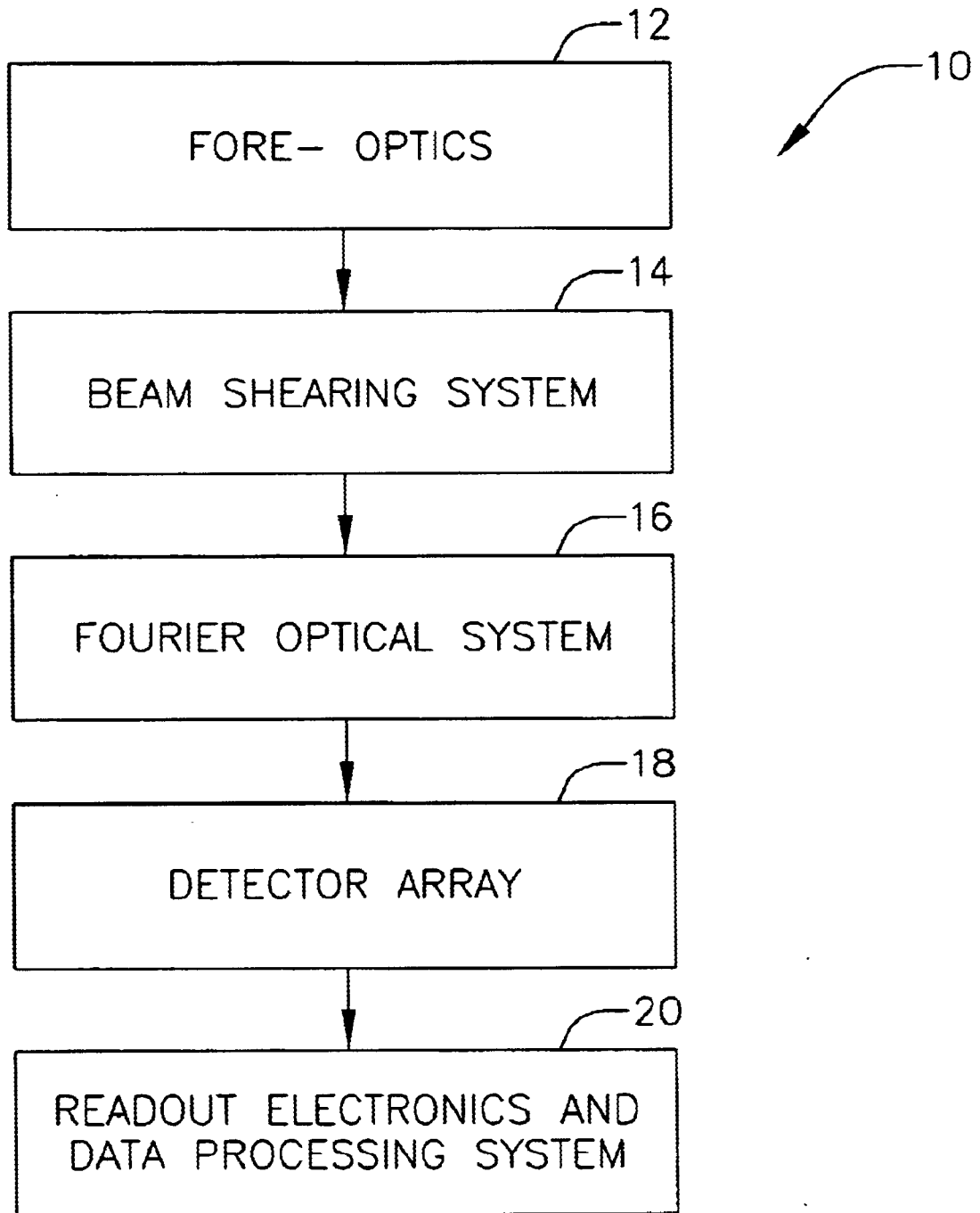
Reininger, Francis; *Near ultraviolet visible infrared mapping spectrometer (NU–VIMS)*; SPIE; 1994; vol. 2209; pp. 332–344.

Reininger, Francis; *VIRTIS: Visible Infrared Thermal Imaging Spectrometer for the Rosetta mission*; SPIE; 1996; vol. 2819; pp. 66–77.

Reininger; Francis et al., *Visible infrared mapping spectrometer–visible channel (VIMS–V)*; SPIE; 1994; vol. 2198; pp. 239–250.
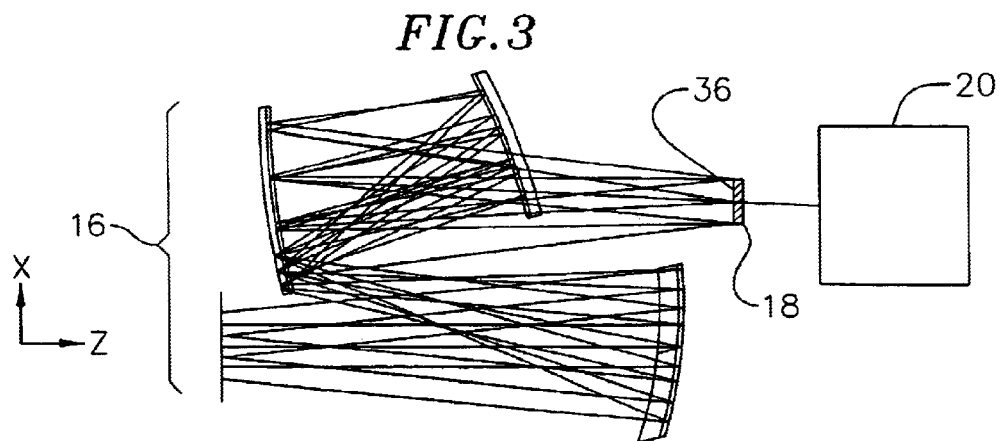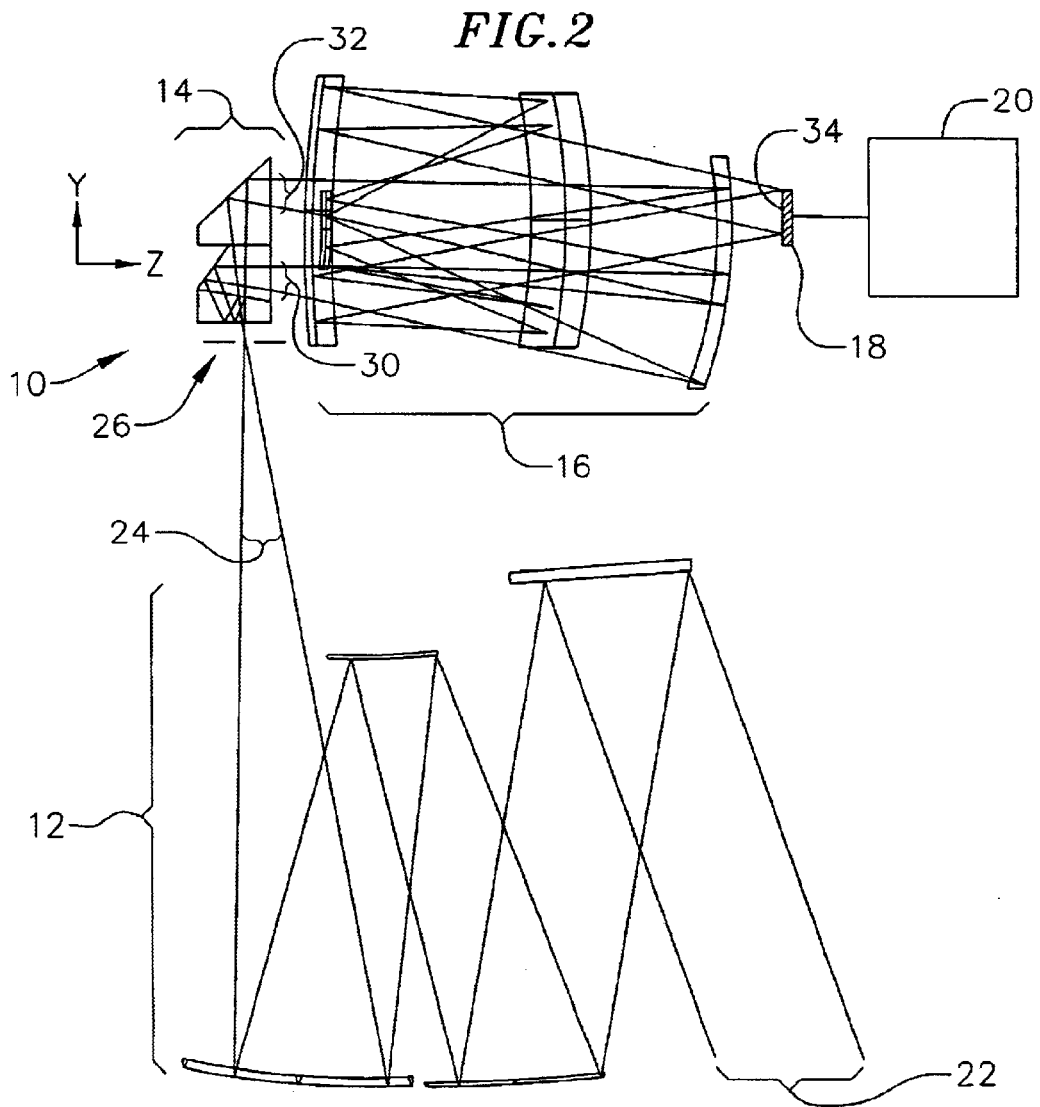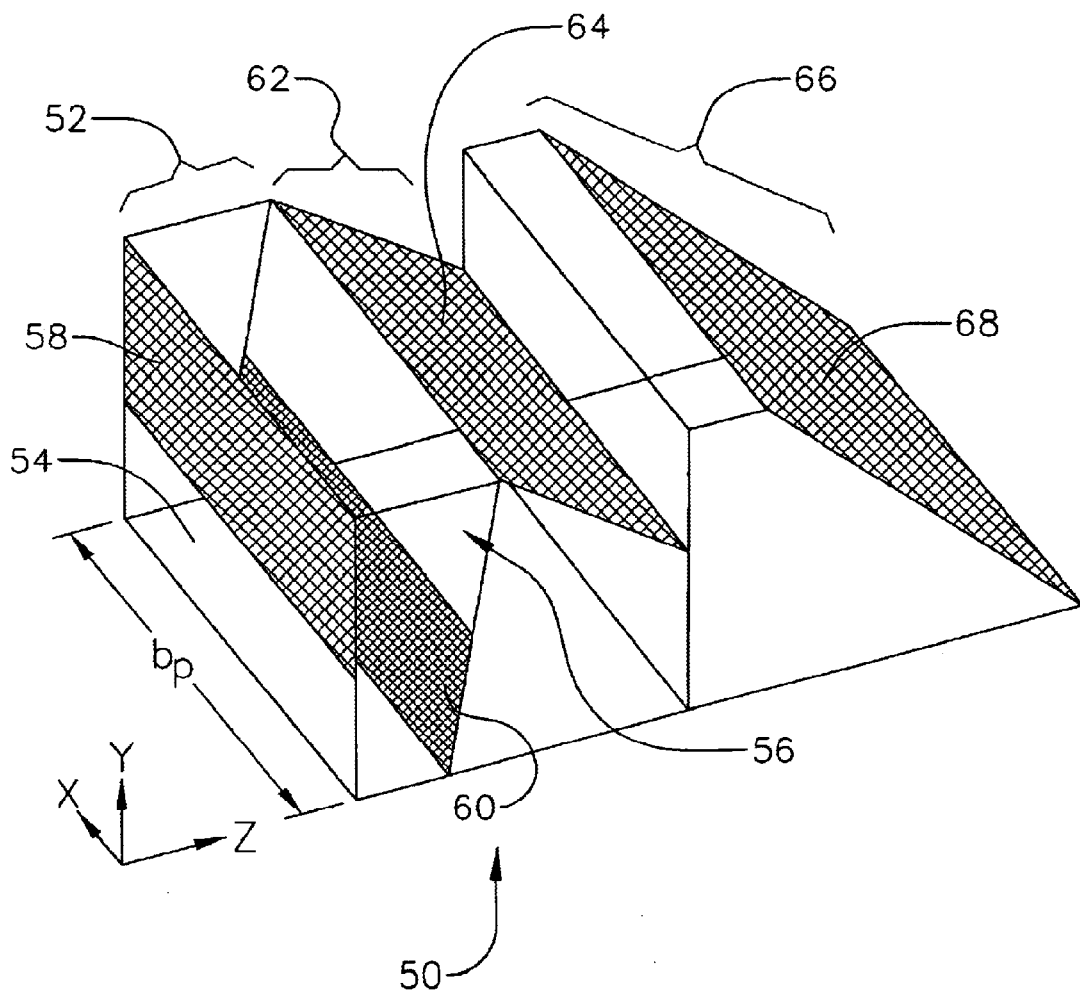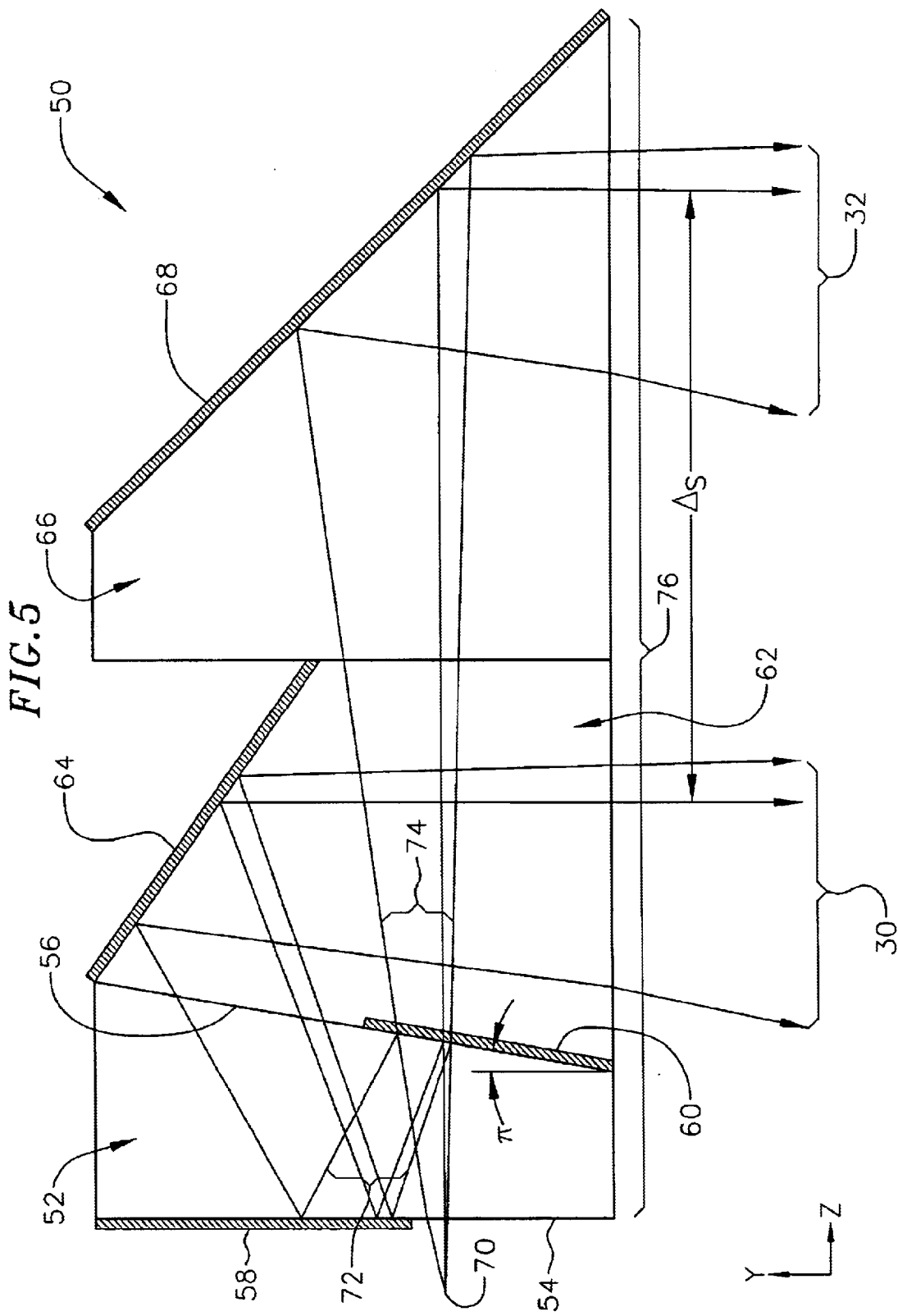
* cited by examiner

FIG. 1

FORE- OPTICS

BEAM SHEARING SYSTEM

FOURIER OPTICAL SYSTEM

DETECTOR ARRAY

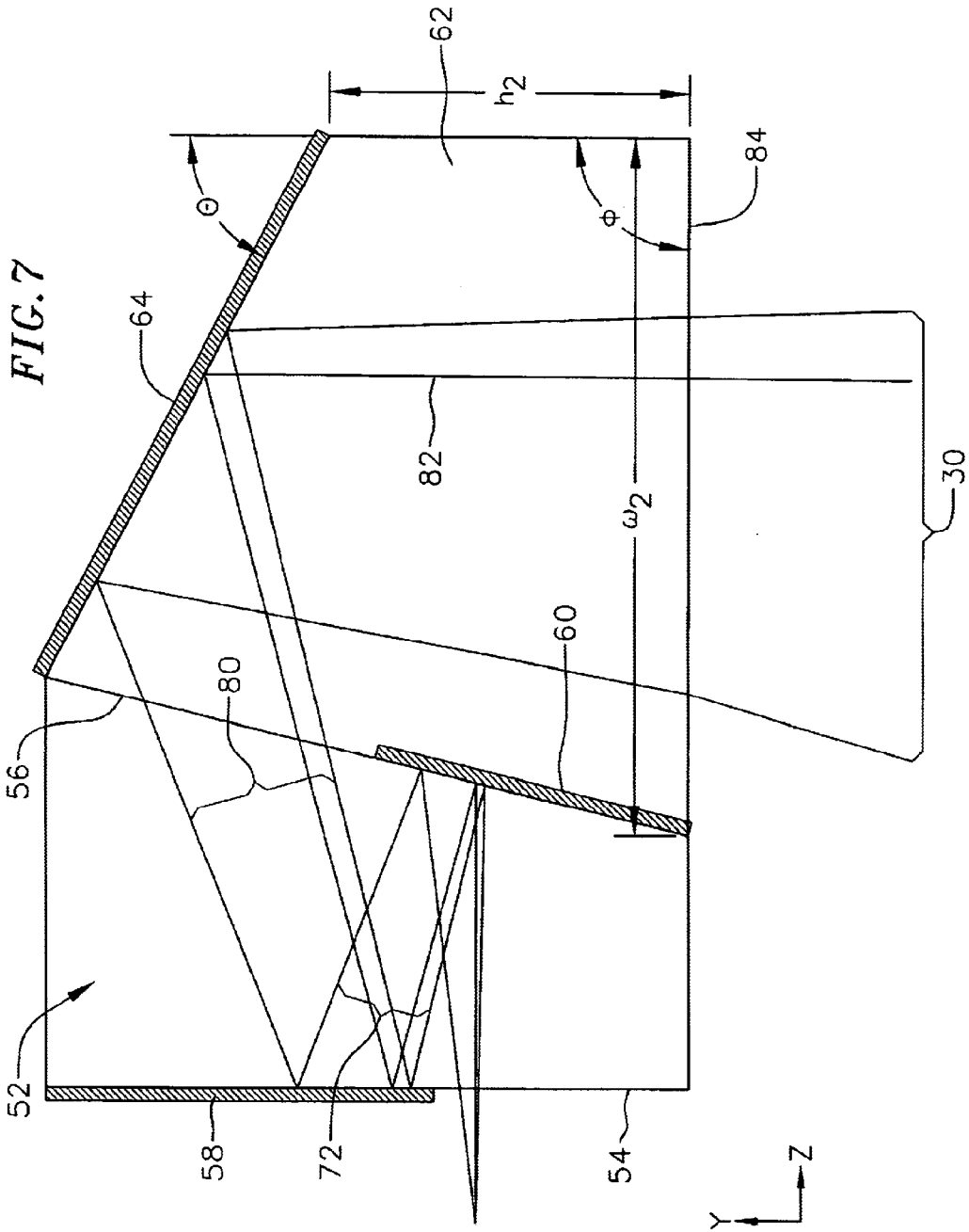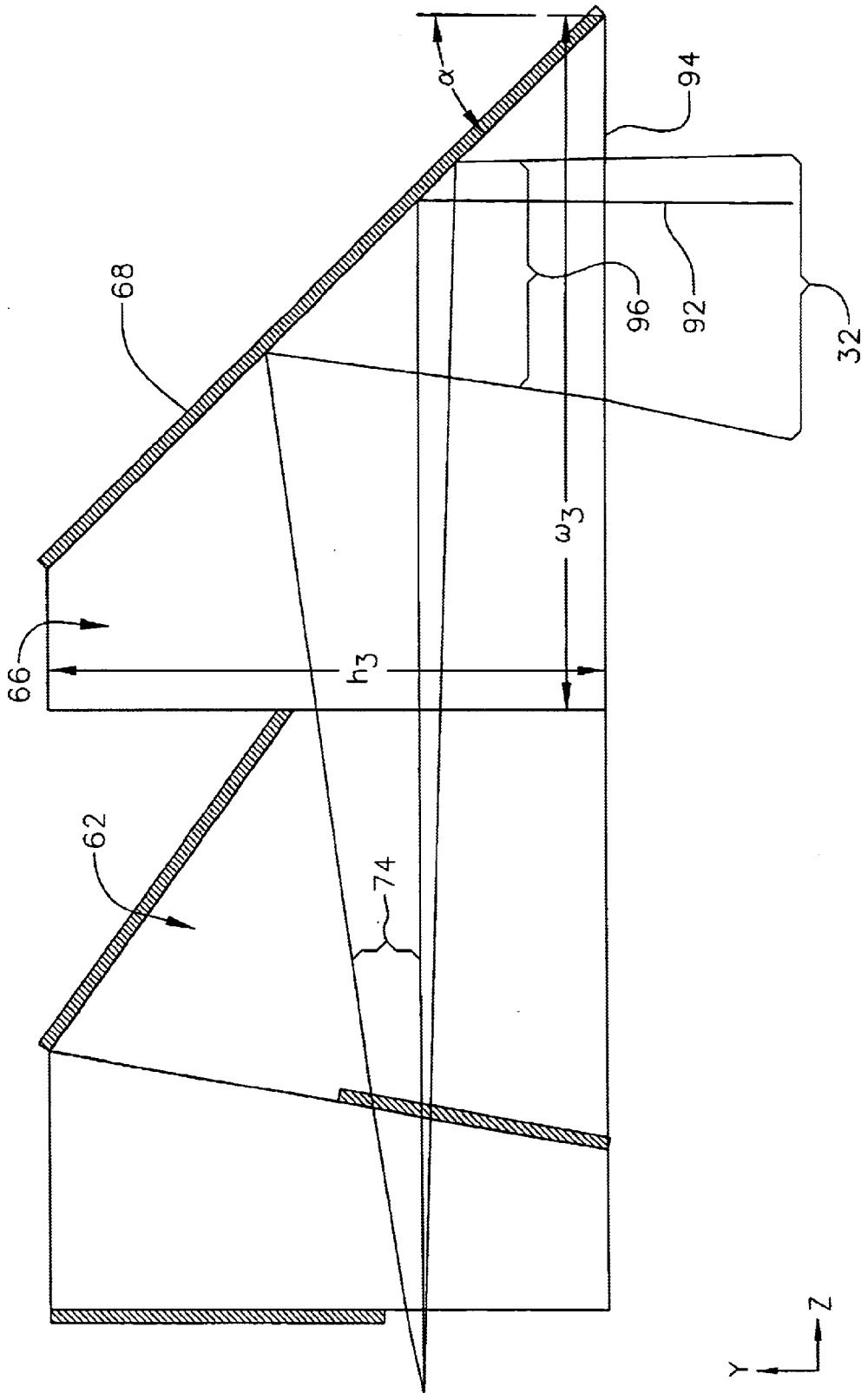READOUT ELECTRONICS AND DATA PROCESSING SYSTEM

FIG.2

FIG.3

FIG.4

FIG.5

FIG.6

FIG.7
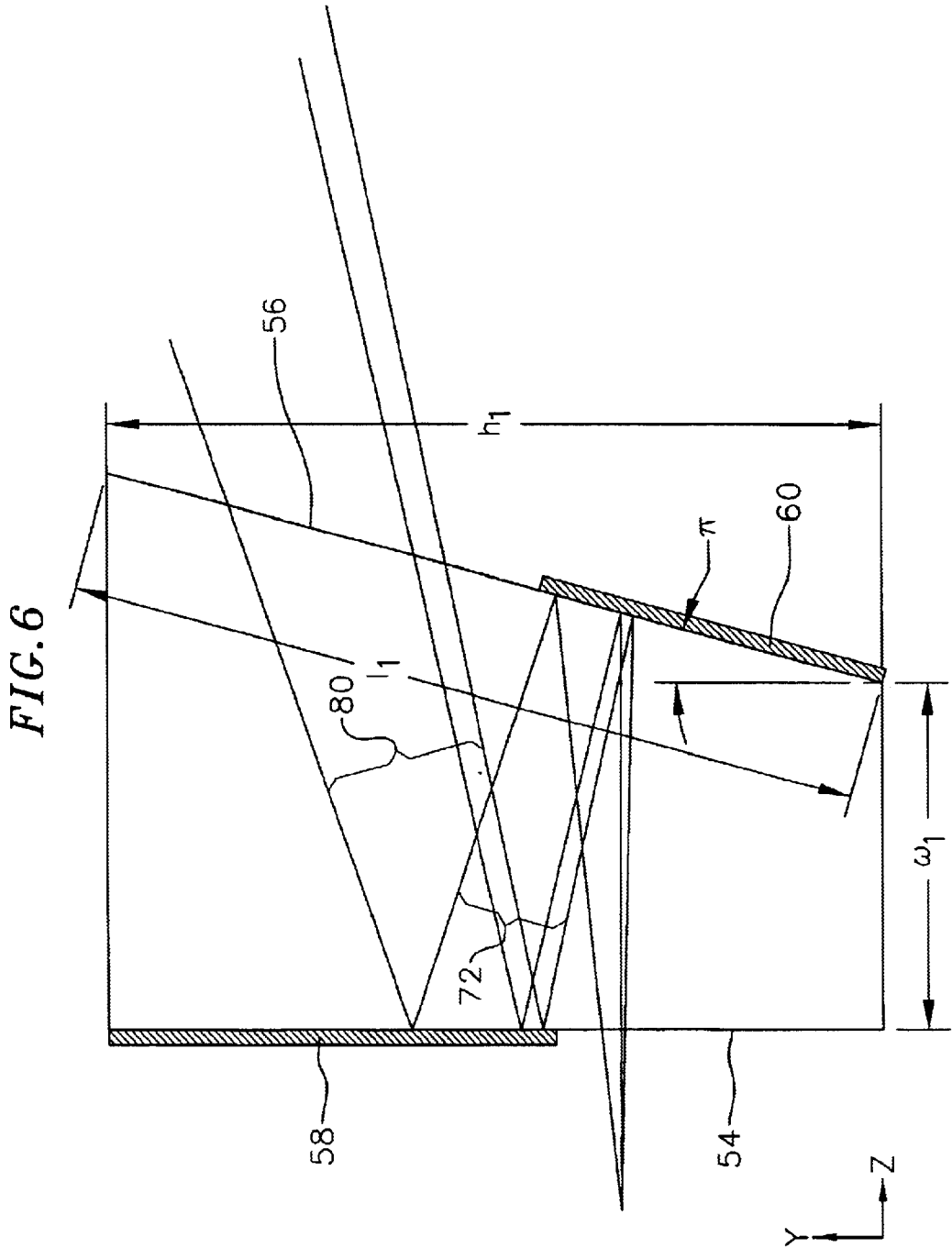
FIG.8

FIG.8A
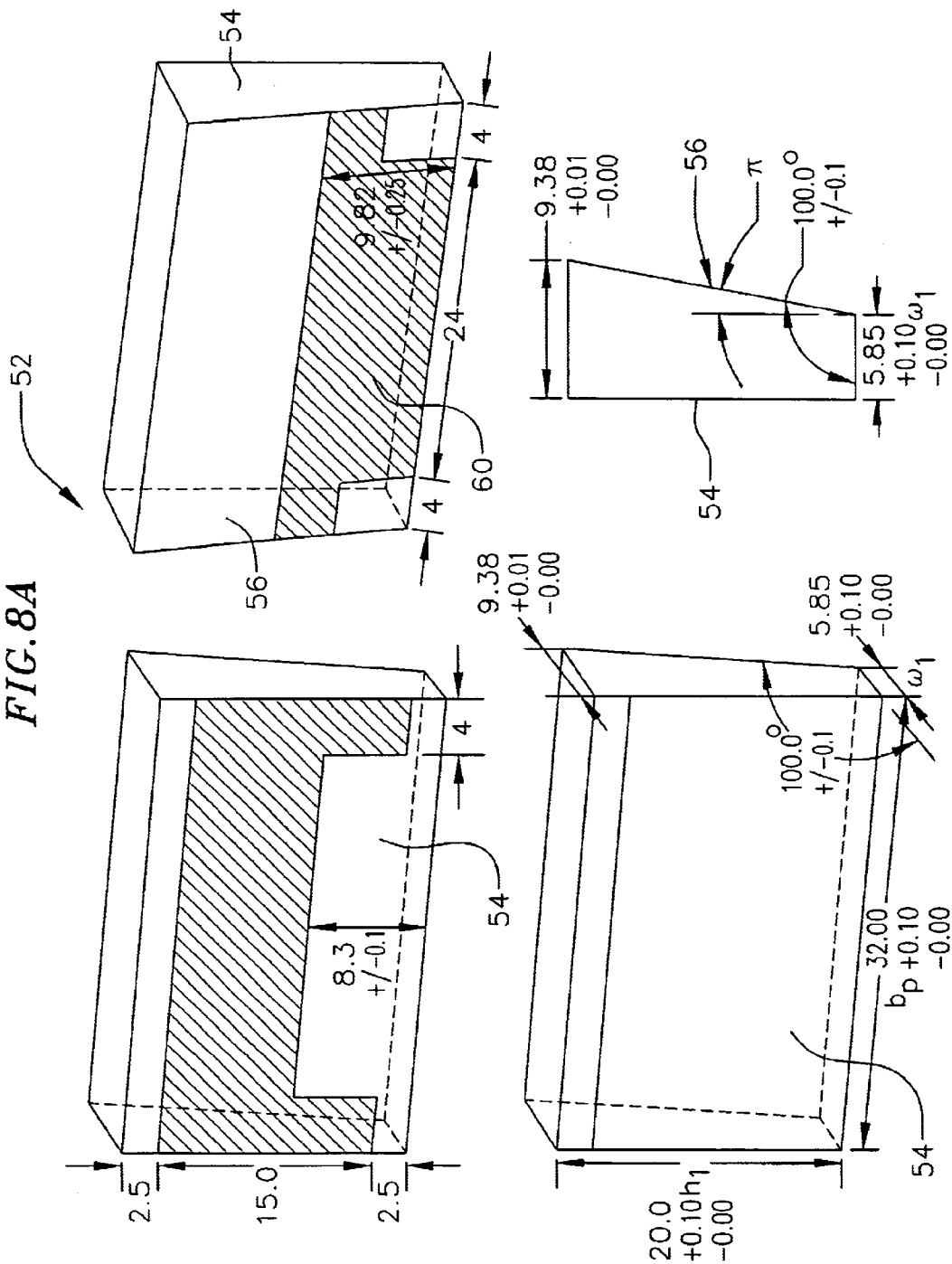
FIG.8B

FIG.9

FIG.10
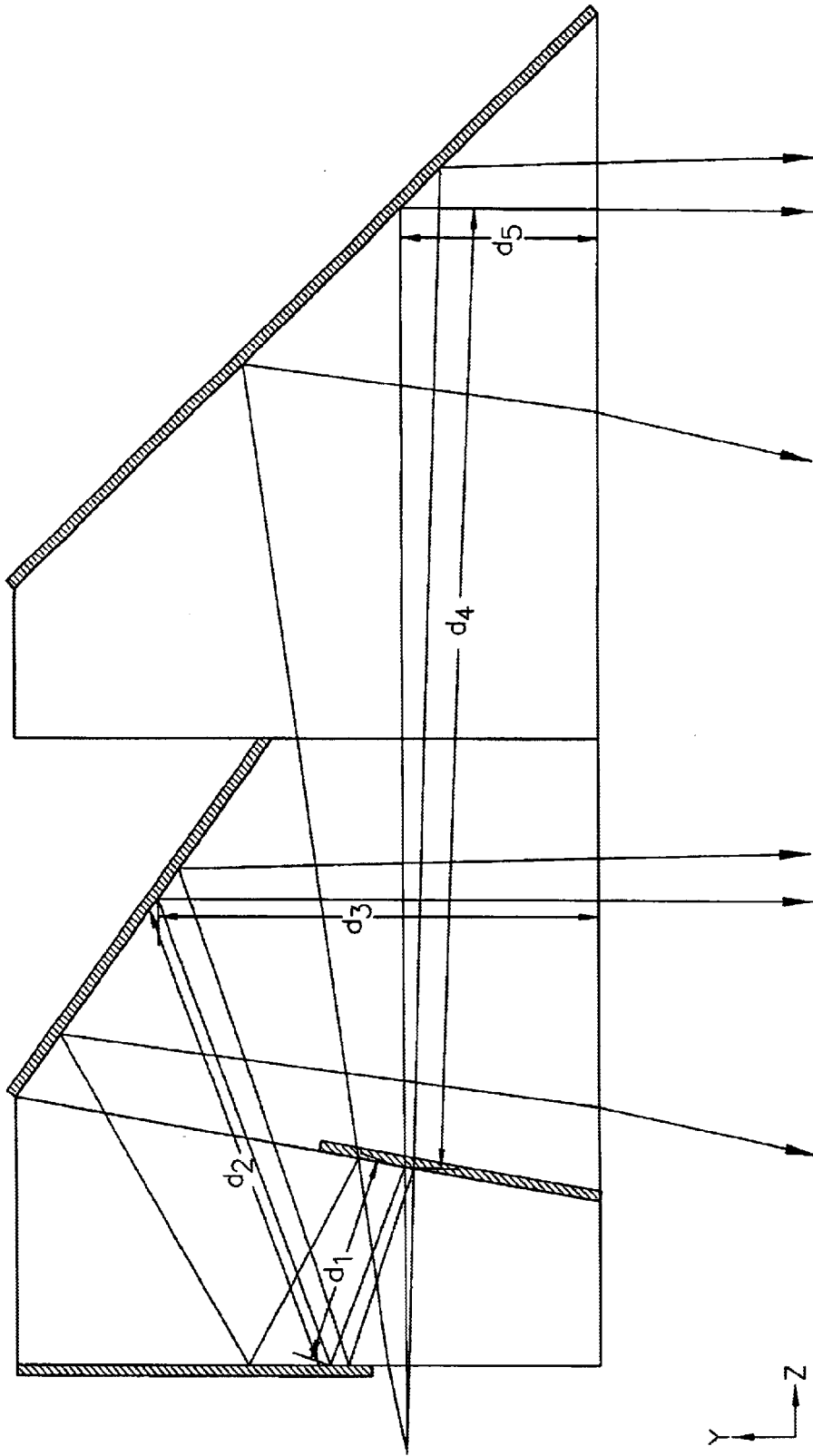
FIG.11
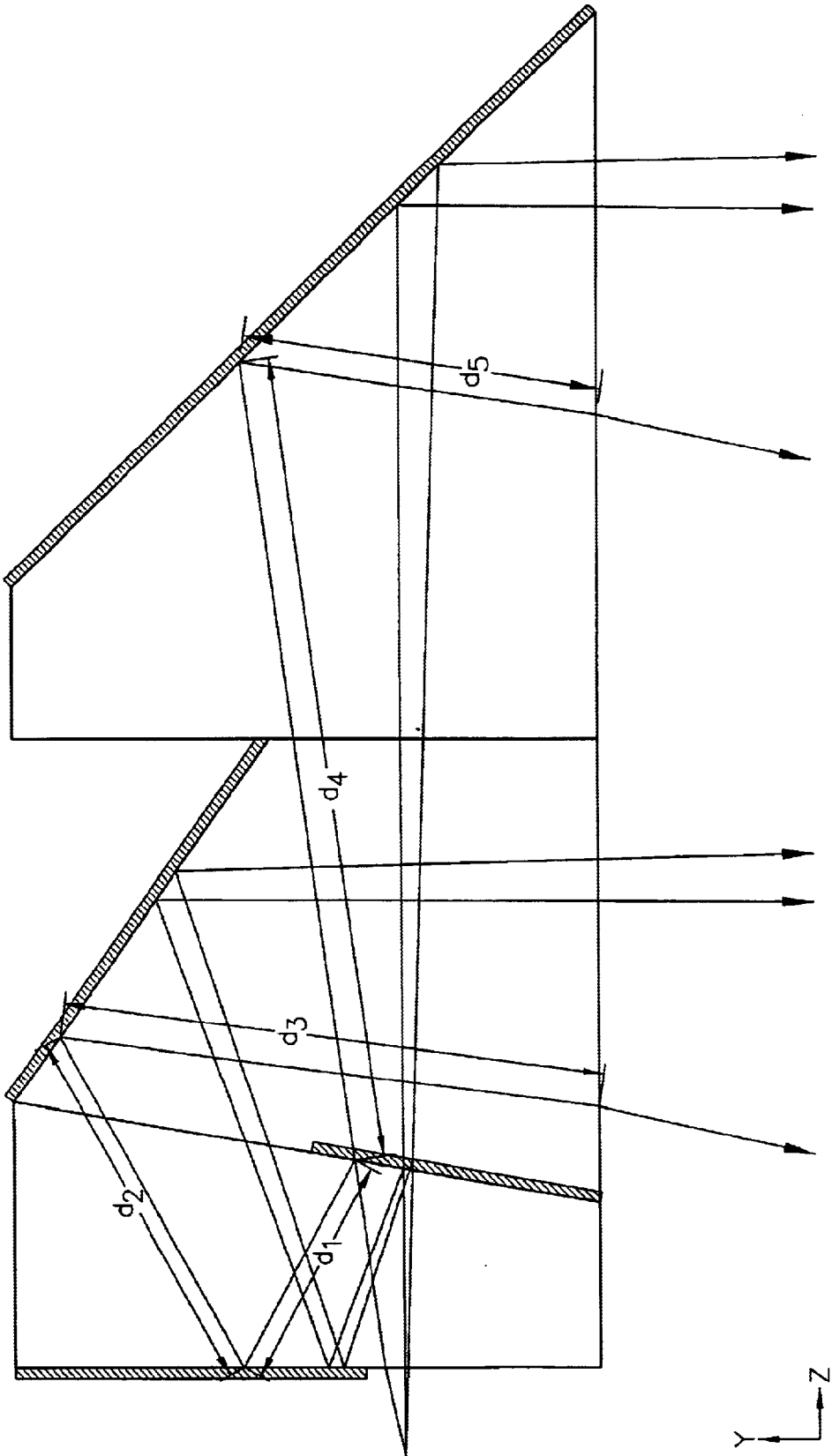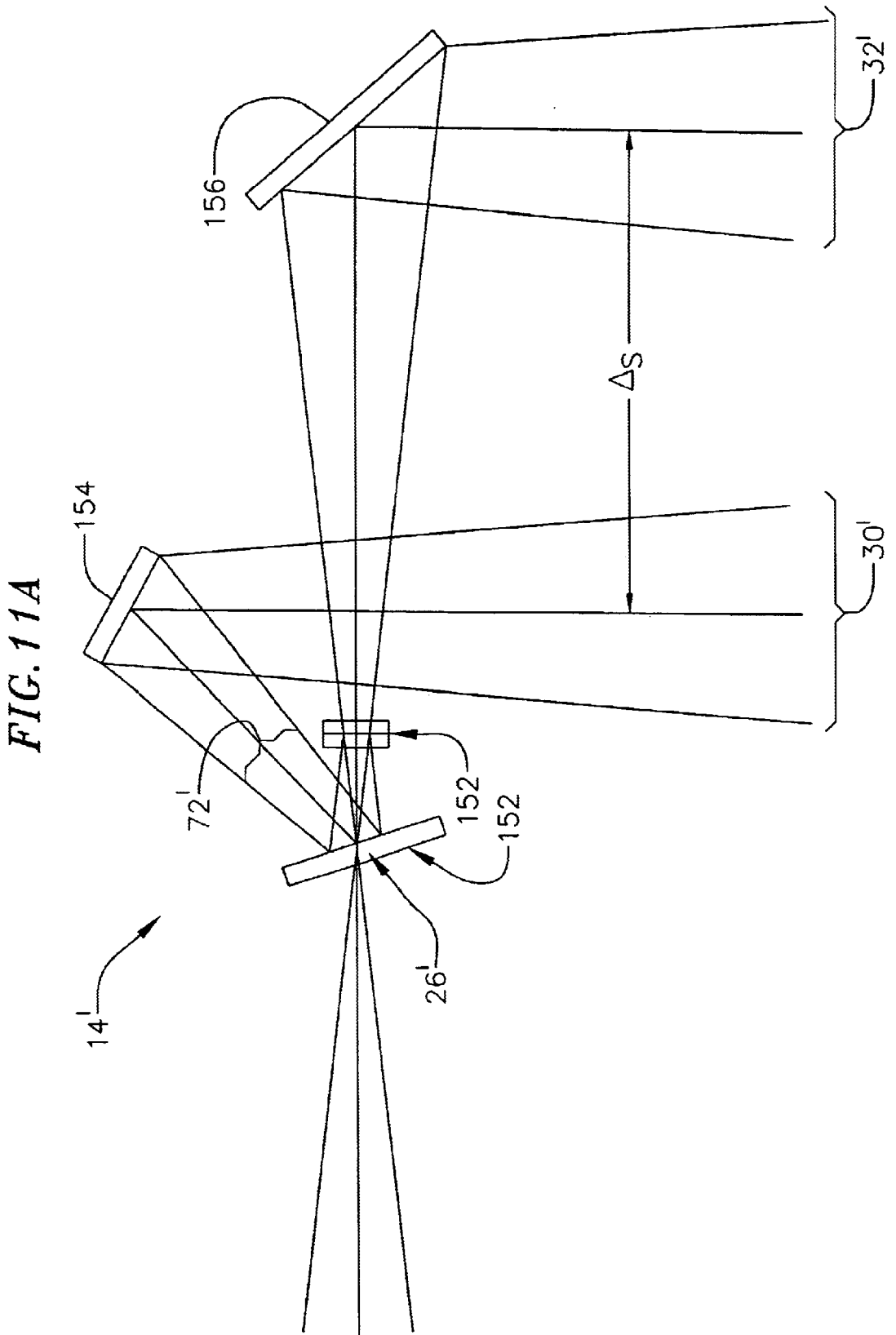
FIG.11A
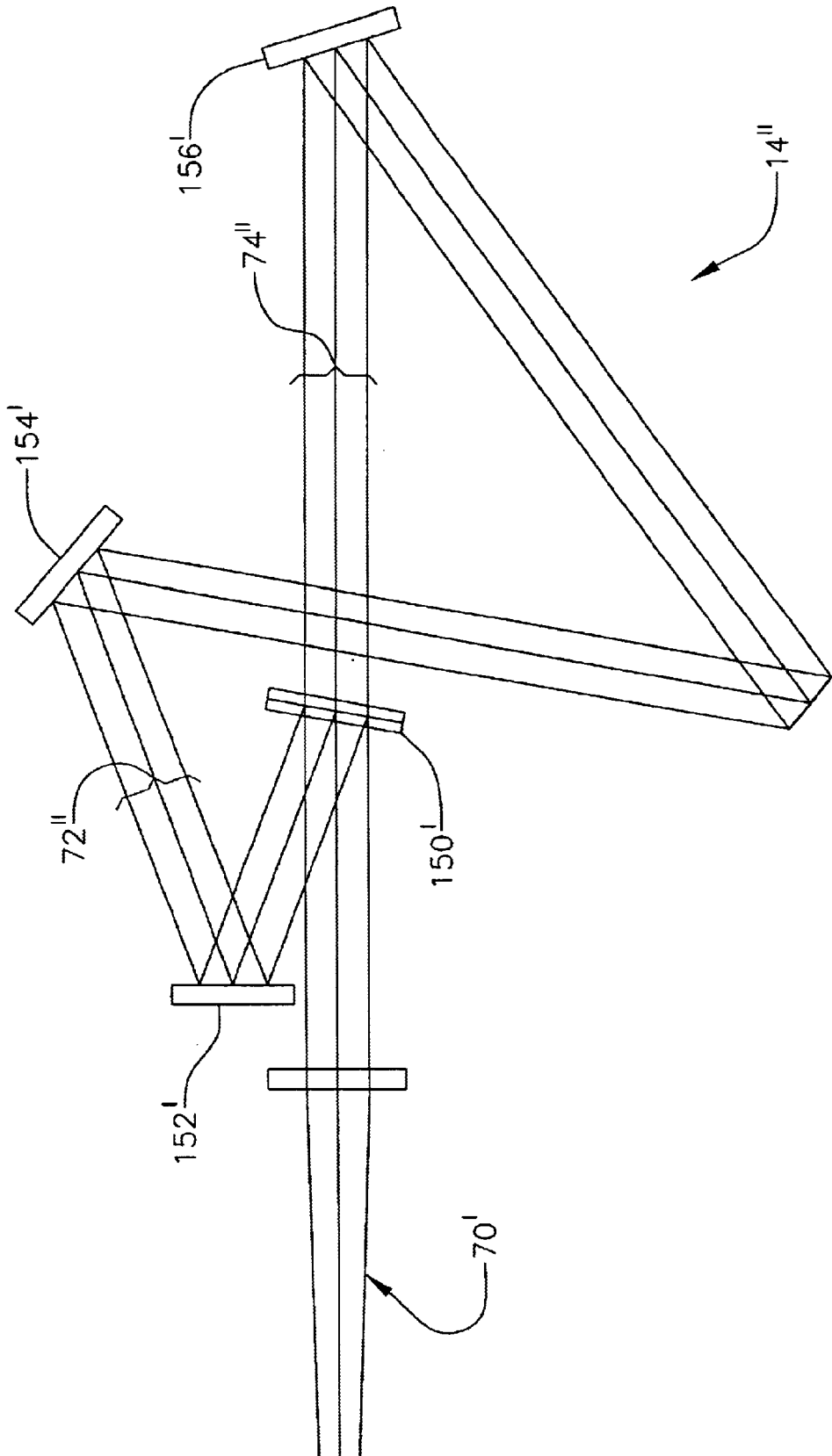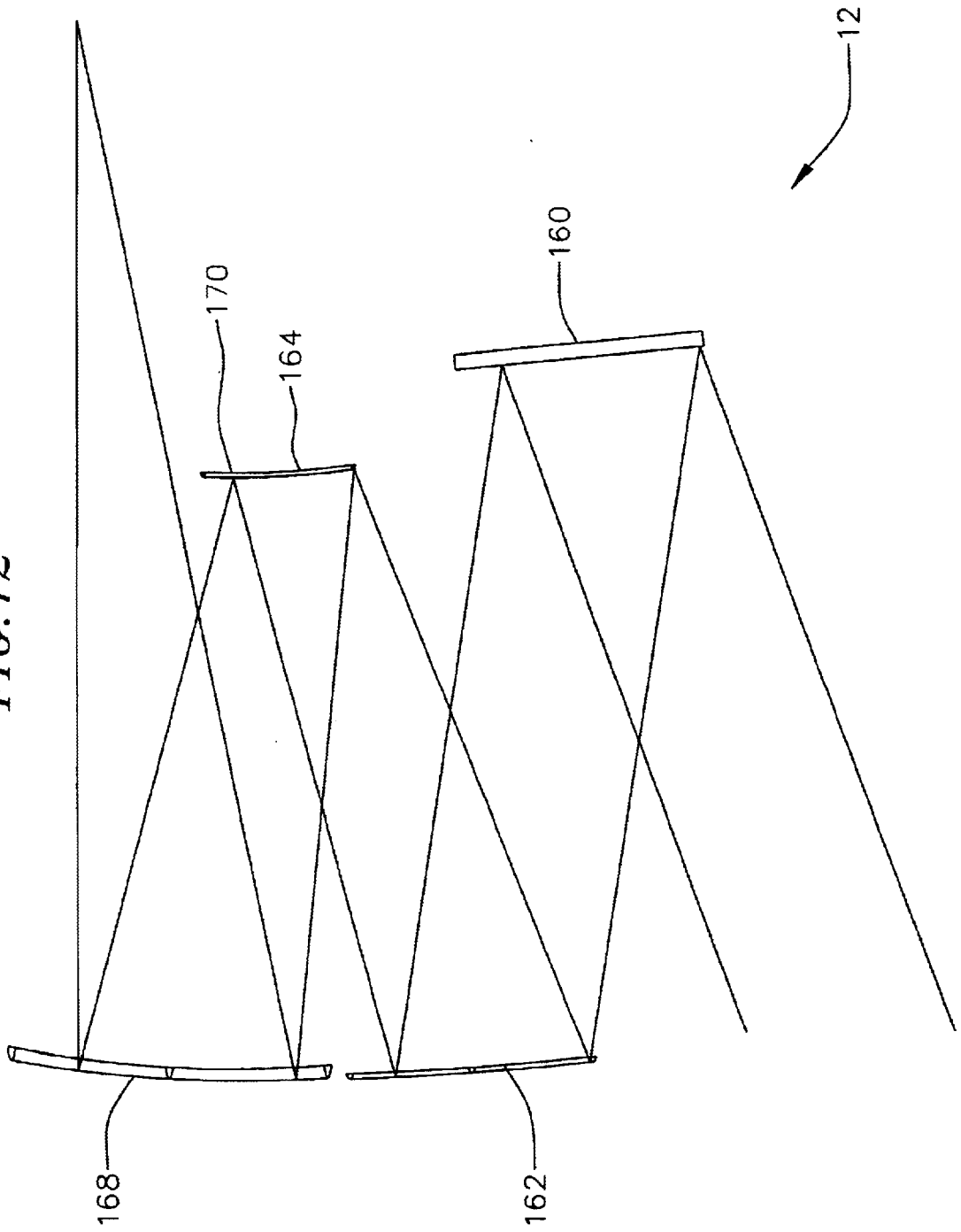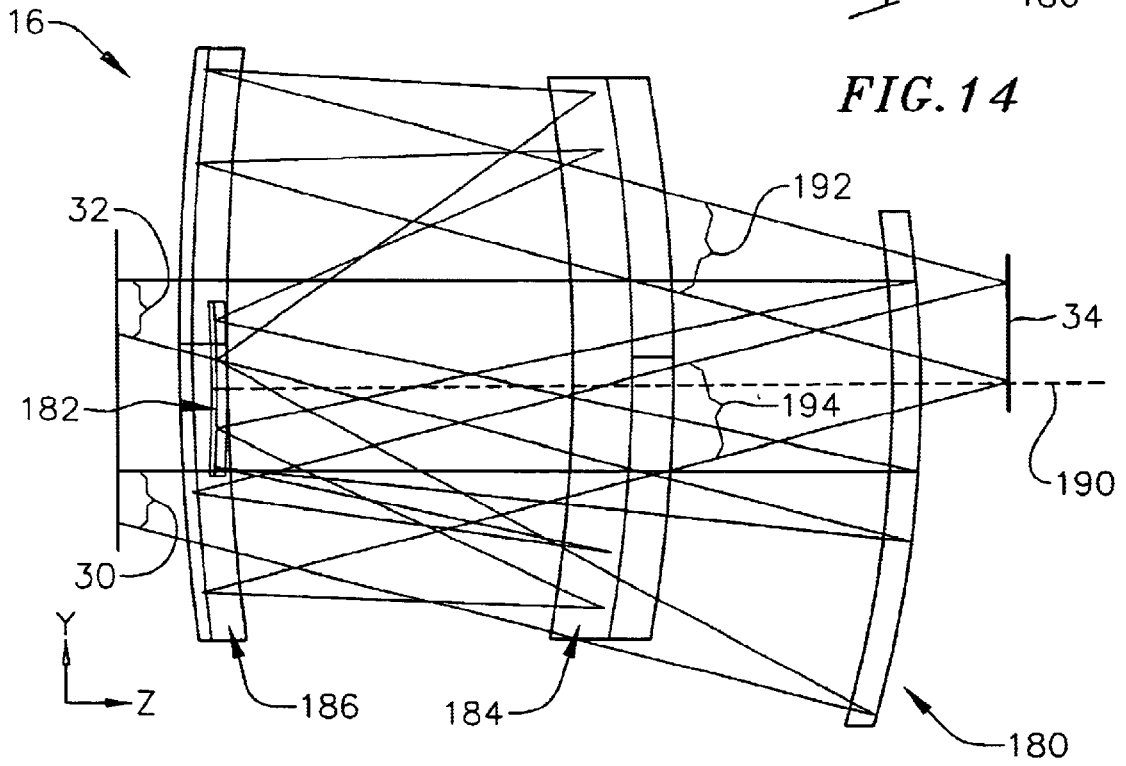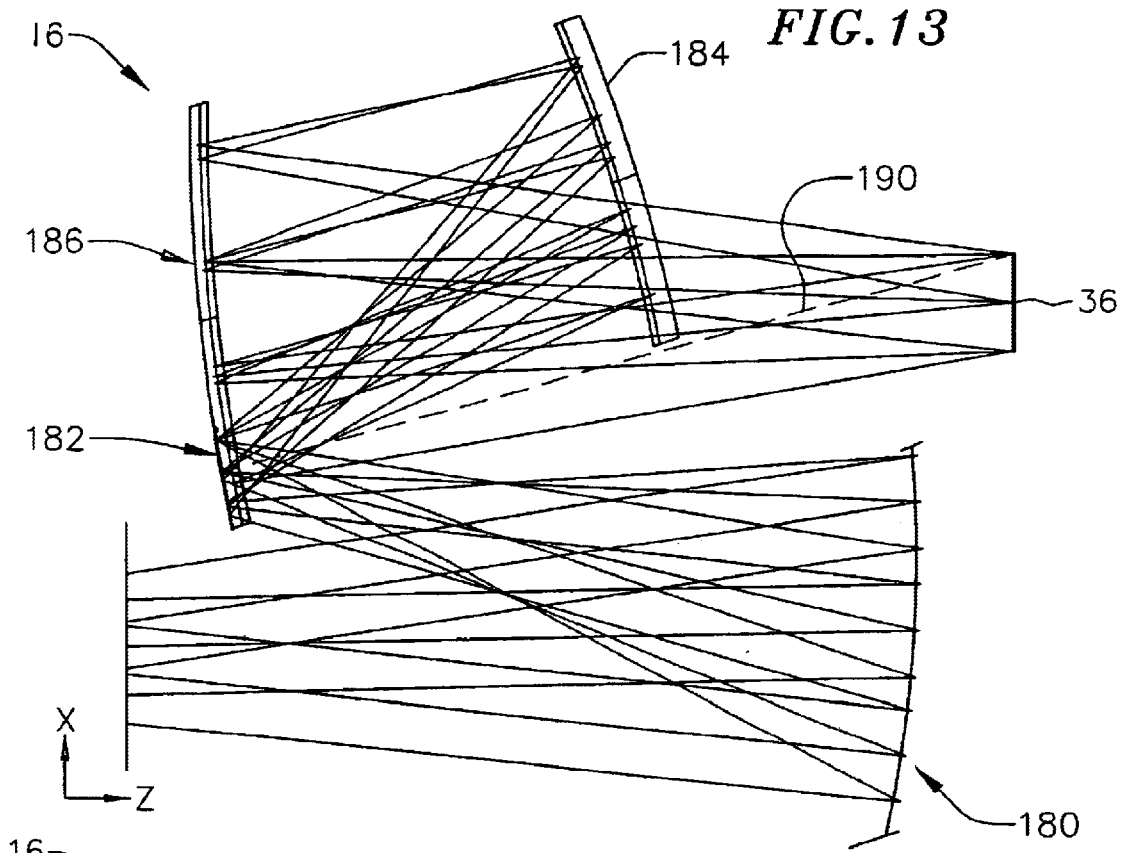
FIG.11B

FIG.12

FIG.13

FIG.14

FIG.15

FIG.16

FIG.17

FIG.18
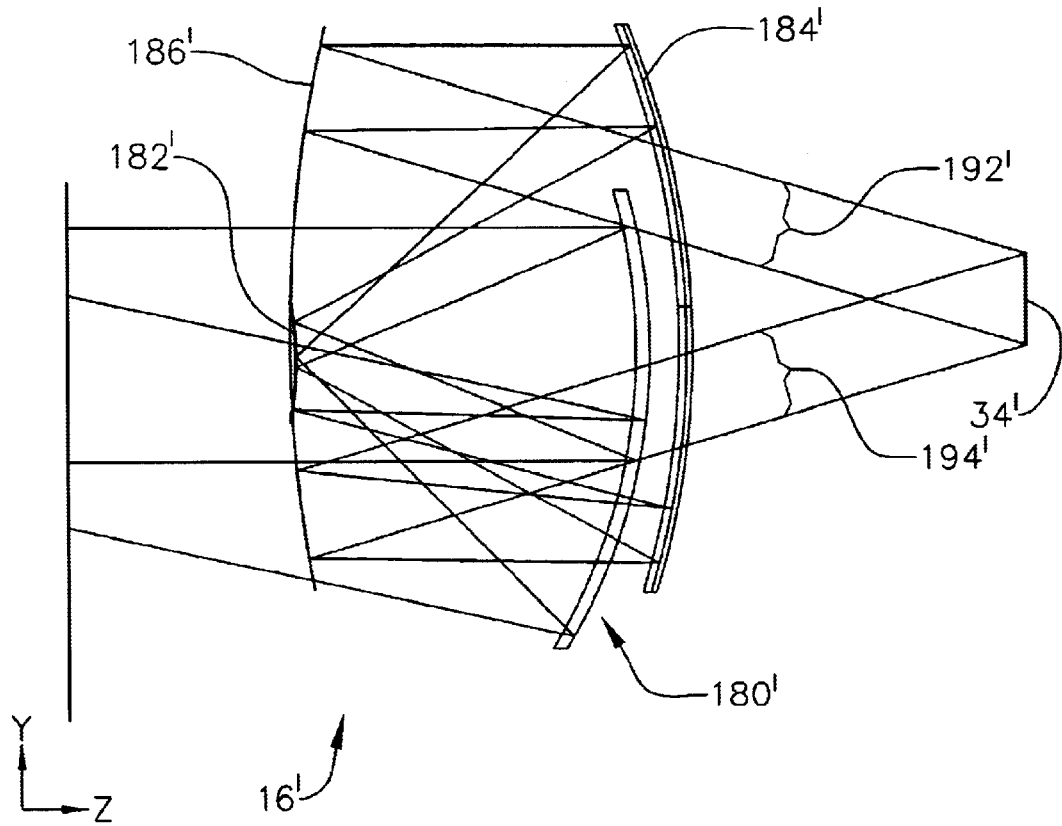
FIG.19

SPATIALLY MODULATED INTERFEROMETER AND BEAM SHEARING DEVICE THEREFOR

CROSS-REFERENCE TO RELATED APPLICATION

This application is based on provisional patent application Serial No. 60/129,383 filed Mar. 13, 1999.

STATEMENT REGARDING FEDERALLY SPONSORED RESEARCH OR DEVELOPMENT

BACKGROUND OF INVENTION

The present invention relates generally to beam shearing systems and their applications, particularly in spatially modulated or static interferometers, which have low volume, low mass, high spectra: resolution, a single instrument line shape function and are field widened.

Interferometers are a class of instruments that convert light from a source into an interference fringe pattern or interferogram. Interferometers make measurements on light within a certain portion of the spectrum. This portion is referred to as the predetermined spectral passband of the interferometer. Frequencies of light outside of the predetermined spectral passband are attenuated so that they do not cause inaccuracies in measurements made by the interferometer.

Spatially modulated or static interferometers use a beam shearing system to shear the input beam into two separate beams and a Fourier optical system can be used to recombine the two sheared beams at a detector array or photographic plate. This procedure generates an optical path difference across the wavefronts of the recombined beams, which results in the formation of a modulation pattern that is fixed in space. If a two dimensional detector array is used, then it can record the spatially modulated pattern as an interferogram in one dimension of the detector array and an image in the orthogonal direction.

Static interferometers are distinguished from other types of interferometers in that they do not require the movement of an optical component or the observational platform to generate an interferogram. Interferometers that require the movement of the observing platform or an optical element to generate their spectrum over a given time interval are prone to unrecoverable spectral errors.

The first reported static interferometer was a Michelson interferometer with tilted mirrors built by G. Stroke and A. Funkhouser (see G. W. Stroke et al., Physics Letters, 1965, Volume 16, Number 3, Pg. 272). Two decades later, T. Okamoto et al used a triangular Sagnac interferometer and a conventional camera lens to generate an interferogram (see T. Okamoto et al., Applied Optics, 1984, Volume 23, Number 2, Pg. 269). In all reported cases, traditional interferom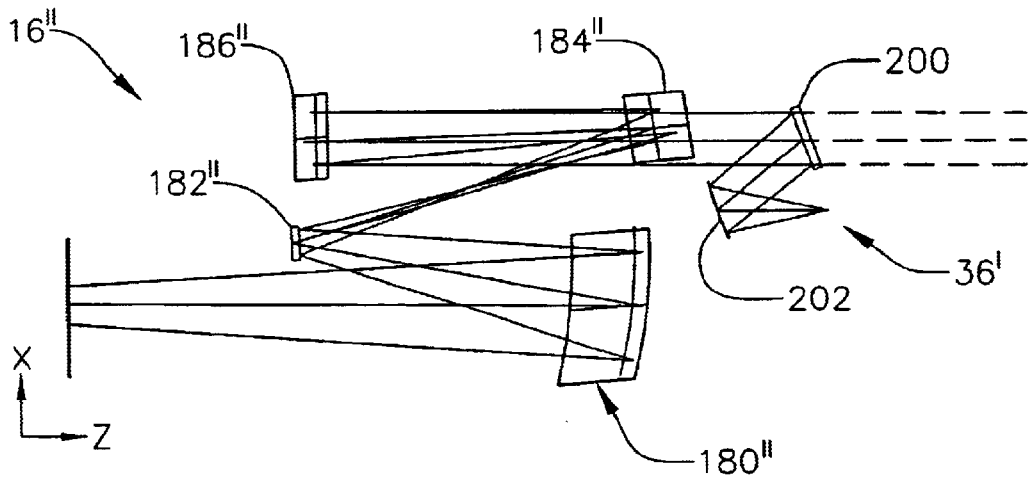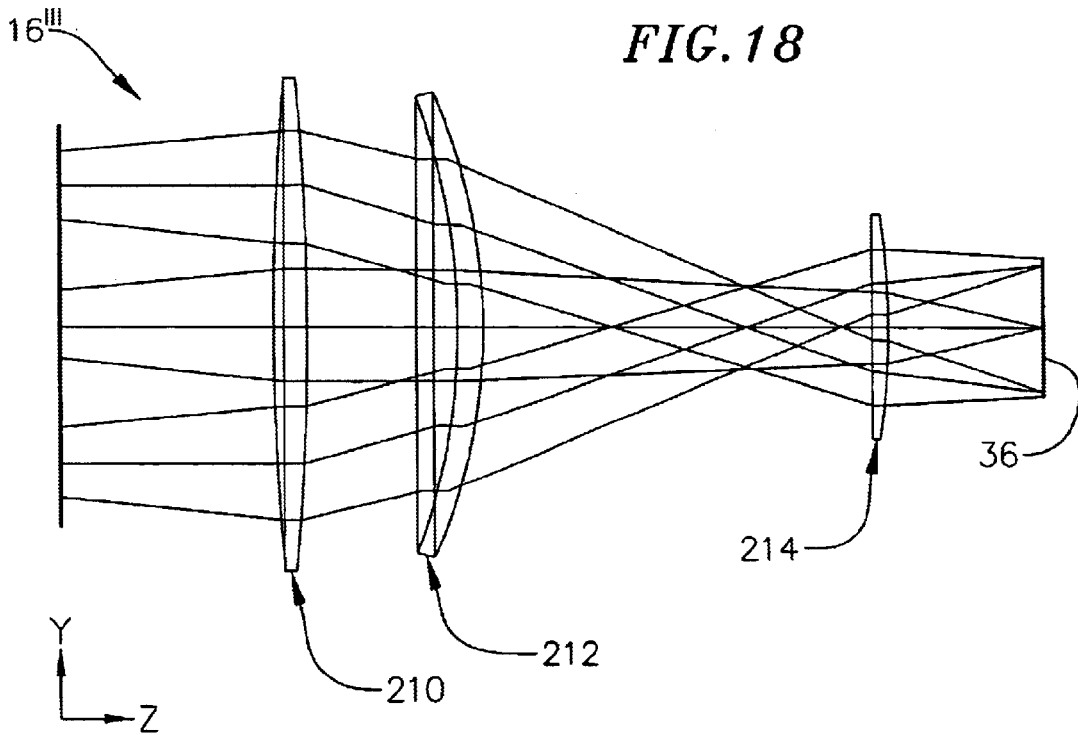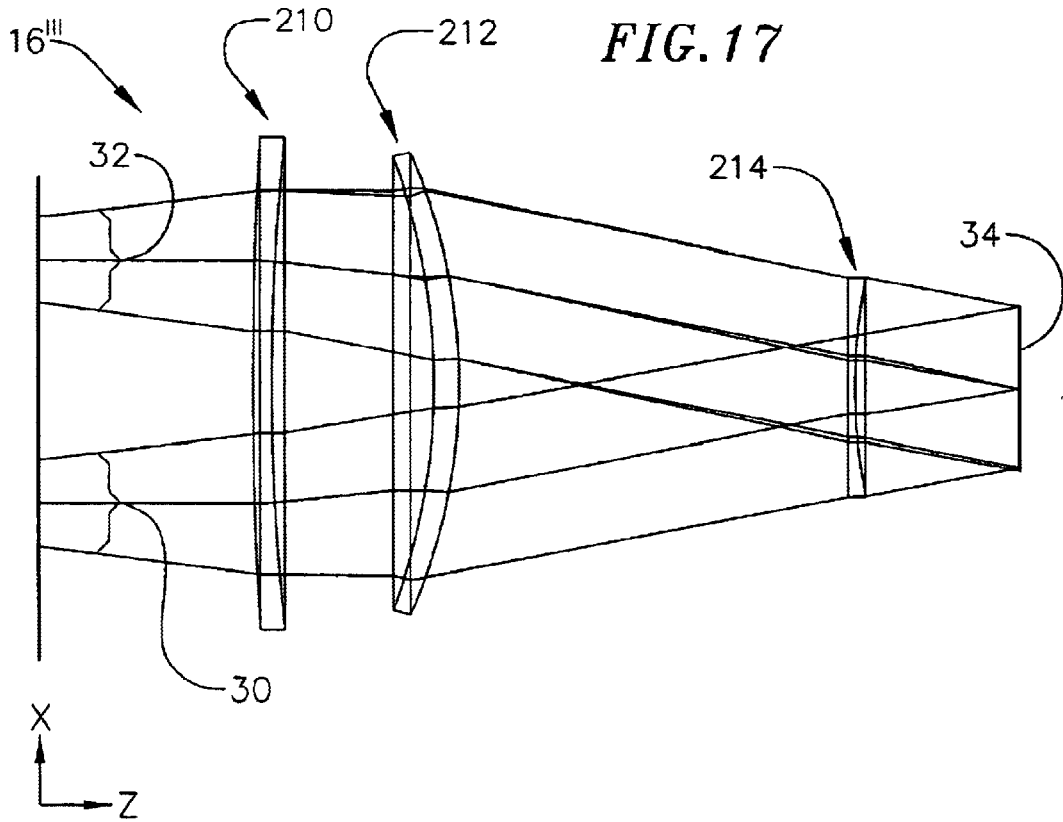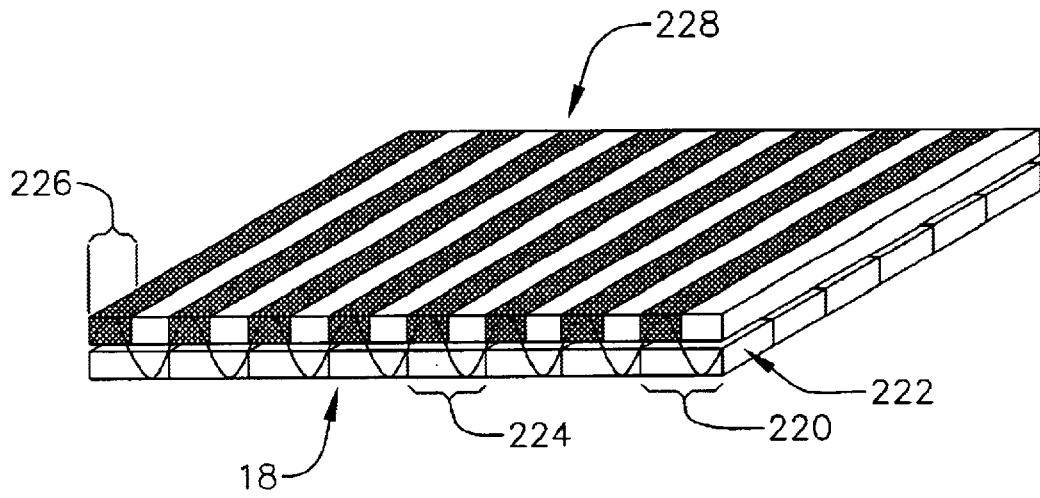eter configurations and conventional Fourier Lenses have been used to generate the interferograms, and the detector arrays have operated in the ultra-violet to near infrared wavelength regimes.

The ability to operate a static interferometer at longer wavelengths than those used by existing static interferometers would offer certain advantages. For instance, operation in the thermal-infrared spectrum would enable fewer pixels to be used to sample the fringes of an interferogram because the frequency of fringes decreases with increased wave-

length. Another advantage of operating in the thermal-infrared spectrum is that the surfaces of the optical components would no be required to meet the stringent surface quality and accuracy requirements of shorter wavelengths interferometers in order to prevent the generation of surface induced fringes that introduce errors by canceling the interferogram fringes. Thus, if a static interferometer were constructed that could operate in the thermal-infrared, then its optical components would be less costly and less time consuming to manufacture.

Conventional interferometer configurations, such as the Michelson and Sagnac interferometers, utilize beam shearing systems that waste at least 50% of the signal. These configurations typically require the beam of light input into the system to make two passes through a beam splitter during the shearing process. Light is therefore reflected back out the entrance through which it entered, resulting in the loss of at least one half of the light entering the static interferometer.

An alternative method that does not rely on the use of a beam splitter to generate a difference in optical path length was described by Padgett et al. U.S. Pat. No. 5,781,293. This method involves polarizing the input bean and then shearing it using birefringent crystals. Despite elimination of the beam splitter, at least 50% of the light entering this type of system is lost due to absorption by the input polariser.

A particular advantage of the Padgett et al static interferometer over other conventional interferometers is that it is field widened. Being field widened means that the slit can be increased to any reasonable width without influencing the spectral resolution. An interferometer will be field widened when it records the interferogram at a pupil plane. At a pupil plane, diffraction does not degrade spectral resolution.

A disadvantage of existing static interferometers is that their physical volume and mass increase significantly when high spectral resolution is required. This greatly increases cost in applications such as remote sensing devices mounted on satellites or space exploration vehicles.

Another disadvantage is that existing static interferometers do not have a single instrument line shape. The instrument line shape is the characteristic shape of the spectrum generated by the static interferometer when the instrument observes a particular frequency of radiation that is substantially narrower in bandwidth than the spectral resolution of the instrument. In existing static interferometers the line shape changes depending on the frequency of the radiation observed. These instruments must be calibrated for the line shape of each frequency in the instrument's bandwidth, which is a time consuming process. Data collected by these static interferometers are difficult to analyze and they are not suitable for generating high spectral resolution output in real time. It is desirable to use a static interferometer that possesses a single instrument line shape and which has near perfect spectral registration. This means that the detector array's output has a single line shape and the lines for the different frequencies are evenly spaced along the spectrum at equal wavenumber intervals. This simplifies the time required to calibrate the instrument and the time required to analyze the data recorded by the instrument.

Accordingly, it is desirable to develop a new static interferometer that is compact, makes use of the majority of incoming radiation, is field widened, can operate in the thermal-infrared region of the spectrum, has a single instrument line shape and has near perfect spectral registration.

SUMMARY OF INVENTION

In one aspect, the static interferometer of the present invention is capable of providing an instantaneous single-

sided interferogram in a tangential exit pupil plane and an image in a sagittal image plane, both of which are located at the same point along the optical axis. The instrument can have an optical efficiency approaching 100 percent, has a high signal-to-noise ratio and is field widened. Because the interferogram is generated at a pupil plane by two perfectly collimated beams, the interferogram is not affected by diffraction. This characteristic enables the instrument to possess spectral radiometric purity, have a very broad spectral bandwidth and have the ability to operate within the thermal-infrared spectrum. In addition, this characteristic enables it to have a single instrument line shape and near-perfect spectral registration. Finally, the instrument is a compact and lightweight unit that is easy to align during construction and simple to calibrate.

In one particularly advantageous embodiment, the fore-optics collect light and focus it onto an entrance slit. The light passes through the entrance slit and into the beam shearing system, which splits it into two separate beams. The beam shearing system is constructed to ensure that the two beams of light emerging from it contain more than 50 percent of the collected light that is within the predetermined spectral passband of the instrument. The emerging beams are incident on a Fourier optical system, which collimates and recombines them onto the exit pupil plane. The recombined beams of light generate an interferogram on a detector line array located at a tangential exit pupil plane, enabling the intensity of the interferogram to be measured by the detector, read out by electronics and then digitized by an analogue to digital converter. The data processing system then manipulates the digital data to extract useful information concerning the spectral composition of the collected light. When fore-optics with a shifted pupil are used, measurements can be made using a single sided interferogram at the tangential exit plane. When a Fourier optical system is used that also focuses the light onto a sagittal image plane located at the same point on the optical axis as the tangential exit pupil plane, then a two-dimensional detector array can then be used to record the intensities of both the image and the interferogram.

The forgoing results are preferably achieved by static interferometers having: fore-optics for collecting light and focusing it into a beam; a spectral resolving system comprising of a beam shearing system to split :he beam of light having a photon flux within a predetermined spectral passband, an optical system for recombining the two split beams onto an exit pupil, and a detector located at the exit pupil. The beam shearing system preferably includes: an entrance slit structure having an entrance slit extending in a first direction for receiving the light collected by the fore-optics; a beam splitter aligned at an angle to the first direction so that the received beam of light is split into two separate beams; a reflective subsystem having a plurality of reflective surfaces defining separate light paths of equal optical path length for the two separate beams, the reflective surfaces arranged such that the two beams contain more than 50 percent of the photon flux that is within the predetermined spectral passband of the collected light. In this embodiment, the chief rays of the two separate beams are also substantially parallel to each other and the two light paths are of substantially equal optical path length.

In one form, the reflective surfaces are also arranged to ensure that the two beams remain substantially in phase relative to one another. In another form, a fore-optics may to have a shifted pupil design to generate single-sided interferograms at the exit pupil plane. In yet another form, the optical system has an optical axis and also recombines the

beams that emerge from the beam shearing system to create a sagittal image plane located at the same point along that optical axis as the tangential exit pupil plane. In yet another form again, the interferometer contains a detector array, read out electronics and data processing system. The detector array records the intensity of the radiation incident on its pixels, the read out electronics digitizes these measurements and transfers them to the data processing system, and the data processing system manipulates the digitized measurements to obtain information about the spectrum of the incident radiation. In a still further form, the data processing system performs Fast Fourier Transforms (FFTs) on the digitized data to obtain the spectrum of the collected light. In a still further form again, the data processing system convolves the digitized data with digital filters to detect the presence or absence in the spectrum of the collected light of frequencies characteristically emitted or absorbed by particular chemicals.

DESCRIPTION OF DRAWINGS

The above and other features of the present invention may be more fully understood from the following detailed description, taken together with the accompanying drawings, wherein similar reference characters refer to similar elements throughout and in which:

FIG. 1 is a simplified block diagram of a static interferometer constructed in accordance with one embodiment of the invention;

FIG. 2 is an optical ray trace diagram of a static interferometer of the type illustrated in FIG. 1, illustrating the Y-Z plane;

FIG. 3 is an optical ray trace diagram of a static interferometer of the type illustrated in FIG. 1, illustrating the X-Z plane;

FIG. 4 is a three dimensional perspective view of a beam shearing system of the type illustrated in FIG. 2;

FIG. 5 is an optical ray trace diagram of a beam shearing system of the type illustrated in FIG. 2;

FIG. 6 is an optical ray trace diagram of the rays reflected by the beam splitting surface of a first prism of the beam shearing system of FIG. 5;

FIG. 7 is an optical ray trace diagram of the path of the first split beam in the first and second prisms of the beam shearing system of FIG. 5;

FIG. 8 is an optical ray trace diagram of the path of the second split beam in the beam shearing system of FIG. 5;

FIG. 8A illustrates the dimensions of the first prism of the beam shearing system of FIG. 5;

FIG. 8B illustrates the dimensions of the second and third prisms of the beam shearing structure of FIG. 5;

FIG. 9 is an optical ray trace diagram illustrating the path lengths of the two beams sheared by the beam shearing structure o the type illustrated in FIG. 2;

FIG. 10 is an optical ray trace diagram illustrating the path lengths of the chief rays of the two beams sheared by the beam shearing structure of the type illustrated in FIG. 2;

FIG. 11 is an optical ray trace diagram illustrating the path lengths of the marginal rays of the two beams sheared by the beam shearing structure of the type illustrated in FIG. 2;

FIG. 11A is an optical ray trace diagram of an alternative embodiment of the beam shearing system illustrated in FIG. 1;

FIG. 11B is an optical ray trace diagram of a second alternative embodiment of the beam shearing system illustrated in FIG. 1;

FIG. **12** is an optical ray trace diagram of fore optics of the type illustrated in FIG. **2**;

FIG. **13** is an optical ray trace diagram of a Fourier optical system of the type illustrated in FIG. **2** (view of the X-Z plane);

FIG. **14** is an optical ray trace diagram of a Fourier optical system of the type illustrated in FIG. **2** (view of the Y-Z plane);

FIG. **15** is an optical ray trace diagram of a first alternative embodiment to the Fourier optical system illustrated in FIG. **1** (view of the X-Z plane);

FIG. **16** is an optical ray trace diagram of a variation on the first alternative embodiment to the Fourier optical system illustrated in FIG. **1** (view of the Y-Z plane);

FIG. **17** is an optical ray trace diagram of a second alternative embodiment to the Fourier optical system illustrated in FIG. **1** (view of the X-Z plane);

FIG. **18** is an optical ray trace diagram of a second alternative embodiment to the Fourier optical system illustrated in FIG. **1** (view of the Y-Z plane);

FIG. **19** is a three dimensional perspective of a detector array of the type illustrated in FIG. **1**, covered by a blocking filter.

DETAILED DESCRIPTION OF THE INVENTION

Referring now to the drawings, FIG. **1** illustrates a static interferometer **10** including fore-optics **12**, a beam shearing system **14**, a Fourier optical system **16**, a detector array **18** and the read out electronics and data processing unit **20**. As shown in FIGS. **2** and **3**, input light **22** is focused by the fore-optics **12** into a beam **24**, which passes through a slit **26** and into the beam shearing system **14**. The beam shearing system **14** splits the beam into two separate beans, **30** and **32**, that are widely spaced when they emerge. These beams **30,32** enter the Fourier optical system **16**, which recombines them to create a pupil plane **34** and an image plane **36**. The detector array **18** is located at the pupil plane **34** and at the image plane **36**. The detector array **18** measures the intensity of the light incident on different areas within the pupil plane **34** and the image plane **36**. These intensity measurements are then recorded by the read out electronics and data processing unit **20**, which performs additional manipulations to extract useful information from the raw measurement data.

The static interferometer **10** of FIG. **1** is preferably fabricated in the configuration shown in FIGS. **2** and **3**, with telecentric fore-optics and a telecentric Fourier optical system. This configuration provides spectral radiometric purity, ensures a single instrument line shape, provides, perfect spectral registration and ensures that the interferometer is field widened.

The performance of the static interferometer **10** is enhanced when the beam shearing system **14** takes the form of a prism structure **50** as illustrated in FIGS. **4** and **5**. This configuration results in an extremely compact form of the static interferometer **10**. The higher the refractive index of the material used to fabricate the prism structure **50**, the more compact the prism's design. The prism structure **50** also possesses characteristics that eliminate dispersion and astigmatism, maximize the efficiency of light utilization and ensure the wavefronts of the two beams emerging from the beam shearing system **30,32** are not out of phase with respect to each other.

The prism structure **50** is typically made of KBr to avoid the need for anti-reflection coatings, but it can also be made

from CsI for very broad spectral bandwidth, from Ge to avoid chromatic defocus and to increase durability, from ZnSe for high durability. Ge and ZnSe require the use of anti-reflective coatings and the performance of CsI is considerably enhanced if antireflective coatings are used. In the illustrated embodiment, all prisms in the prism structure **59** are made from the same material to ensure that both the beams emerging from the beam shearing system **30,32** travel through optical paths of identical length.

Considering the prism structure **50** of FIG. **4** in further detail, the first prism **52** consists of an entrance surface **54** and a beam splitting surface **56**. A portion of the entrance surface **54** is covered in a reflective coating **58** and a portion of the beam splitter surface **54** is covered in a beam splitter coating **60**. The second prism **62** and third prisms **66** each have a surface that is completely coated in a reflective coating **64** and **66**. All other surfaces in the prism are optically transparent. The reflective coatings of the prism structure **50** are typically made from Al, Au or Ag and the beam splitter coating **60** is usually made from Ge.

The material chosen to construct the prism structure illustrated in FIG. **4** effects the optical efficiency of the beam splitter. The variation in optical efficiency with the choice of material is demonstrated by TABLE 1A.

TABLE 1A

PRISM EFFICIENCIES AT 10 μm WAVELENGTH.			
Substrate/Coating	Ge + Al[1]	Ge + Al + Protective[2]	Ge + Au + AR[3]
KBr	80%	85%	95%
CsI	72%	80%	95%
ZnSe	—	—	91%
Ge	—	—	90%

NOTE 1: "Ge + Al" implies a germanium beam splitter plus aluminum coatings on all reflection surfaces. No coatings are placed on transmission surfaces.
NOTE 2: "Ge + Al + Protective" implies a germanium beam splitter coating, aluminum reflection coatings, and protective coatings on all transmission surfaces. The protective coatings protect the water-soluble salt crystals from moisture.

NOTE 3: "Ge+Au+Ar" implies a germanium beam splitter coating, gold reflection coatings, and anti-reflection coatings on transmission surfaces. The gold coatings require an adhesive layer. No germanium beam splitter coating is required for the germanium substrate. The AR coatings on the salt crystals are assumed to be narrow-band, and the AR coatings on the metallic substrates are assumed to be broadband.

A closer examination of FIG. **5** demonstrates how the prism structure **50** shears the input beam **70** of FIG. **5** into two separate beams **72** and **74**. The input beam **70** enters the prism through the entrance surface **54** and is incident upon the beam splitter coating **60**. This splits the beam and approximately 50% of the light is reflected in a first split beam **72** and the remainder of the light is transmitted in a second split beam **74**. It is advantageous for the prism structure to be manufactured with the beam splitting surface **56** having a minimal tilt relative to the entrance surface **54**, shown as π on FIG. **5**. This improves the efficiency of the beam splitting coating **60**, reduces polarization and prevents the first split beam **72** from being totally internally reflected at the air gap between the beam splitter surface **56** and the second prism **62** by the beam reflected off the reflective coating on the entrance surface **58**.

The first split beam **72** is reflected by the reflective coating on the entrance surface **58** and is then reflected again by the second prism's reflective surface **64**. The first split beam **72**

then exits the prism structure **50** through the exit surface **76**. The second split beam **74** continues until it strikes the third prism's reflective surface **68**, where it is reflected and exits the prism structure **50** through the exit surface **76**. The surfaces of the prism structure are arranged so that the first split beam of light **72** and the second split beam of light **74** have traveled the same optical distance and are parallel when they exit the exit surface **76**. Overall, the prism structure **50** is extremely efficient in its utilization of light. The only way that light entering the system through the entrance surface **54** can exit the prism structure **50** is through the exit surface **76**.

The prism structure **50** reflects the first split beam **72** three times and the second split beam **74** only once ensure that the wavefronts of the two beams do not undergo a 180° phase change with respect to each other. If the two wavefronts are in-phase, then the image is preserved across the entrance slit **26**, single sided interferograms can be generated without loss of signal, and the optical aberrations generated by the Fourier optical system **14** tend to cancel out when the two beams **30,32** recombine at the detector array **18**.

The shape of the prism structure **50**, as shown in FIG. **4**, affords easy mounting and alignment. Proper alignment of the prisms is important because it ensures that the modulation efficiency of the interferometer is maximized. The modulation efficiency is a measure of the fringe visibility or contrast and directly affects the signal amplitude. When the chief rays emerging from the prism are not parallel to each other or the optical system is not telecentric, then the modulation efficiency, $\eta(\beta)$, decreases as a function of the angle, β, between the two chief rays.

Therefore, a special mounting system (not shown) manufactured from aluminum is used that hard mounts the prisms **52,62,66** without the need for epoxies. The prisms are held in aluminum caps that are held in place by springs. The springs hold the prisms in alignment when the spectrometer temperature is reduced. The air gaps between the prisms are not sealed with adhesives because this introduces strong absorption features in the thermal infrared region of the spectrum.

A closer examination of FIGS. **5** through **11** reveals how the prism structure **50** is manufactured to ensure that it possesses the properties necessary for it to function effectively as the beam shearing system **14** in the static interferometer **10**. Three requirements apply to the construction of all of the three prisms **52,62,66**. The first is that the prism structure is constructed so that the entrance surface **54** is substantially perpendicular to the chief ray of the input beam **78** and the exit surface **76** is substantially perpendicular to both chief rays of the exit beams **30** and **32**. The purpose of constructing the prism structure **50** in this way is to eliminate dispersion and astigmatism. Dispersion alters the instrument line shape as a function of wavenumber and astigmatism creates different wavefront errors in each of the two exit beams **30** and **32**, broadening the instrument line shape. The following equation and explanation illustrates the effect of astigmatism on the instrument line shape. Let $\Delta\epsilon$ represent the difference in wavefront errors between the two beams at the exit pupil. Wavefront errors are caused by optical aberrations. If the optical aberrations or wavefront errors of the two beams are identical and vary slowly across the wavefront, then there is no influence on the spectral resolution or instrument line shape. Astigmatism would cause a difference in wavefront errors between the two beams. For a given $\Delta\epsilon$, the width of the instrument line shape at half maximum, $\Delta V_{1/2}$, will increase according to the following equation:

$$\Delta v_{1/2} = \frac{0.605}{\delta_{max}} + \frac{1}{y_{max}}\sqrt{\frac{v\Delta\varepsilon}{2\cos\left(\frac{FOV_F}{2}\right)}\left\{\left[\frac{F}{\Delta S\cos\left(\frac{FOV_F}{2}\right)}\right]^2 - \frac{1}{4}\right\}}$$

where

ΔS is shown on FIG. **5**

F is the focal length of the Fourier Lens,

δ_{max} is the maximum optical path difference,

Y_{max} is the distance between the center of the exit pupil and the edge of the exit pupil,

and

$FOV_F = 2\arctan(\Delta S/2F)$ is the field of view of the Fourier Lens.

The second is that the breadth of each of the prisms **52,52,66**, shown as b_p on FIG. **4**, must be large enough so that all the light entering through the length of the slit is contained within the prism. In addition to these two requirements, there are manufacturing requirements that apply to each of the prisms **52,62,66** individually. The third is that the entrance surface must be perpendicular to the exit surface to minimize optical aberrations.

A closer examination of FIG. **6** demonstrates that the first prism **52** is manufactured so that its shape ensures the following. Firstly, the portion of the entrance surface **54** that is not coated is large enough to ensure that none of the input beam **70** is incident upon the portion of the entrance surface that is coated in reflective coating **58**. Secondly, the portion of he beam splitting surface that is coated in a reflective coating 6C is wide enough to ensure that none of the input beam **70** is incident on the portion of the beam splitting surface **56** that is not coated in beam splitting coating. Thirdly, the width of the first prism w_1, the height of the first prism, shown as h_1, on FIG. **6** and the tilt angle of the beam splitting surface relative to the entrance surface, shown as π on FIG. **6**, ensure that the entire first split beam **72** is incident on the portion of the entrance surface **54** that is coated in reflective coating. Fourthly, the width of the first prism w_1, the height of the first prism h_1, the tilt angle π and the length of the beam splitting surface **56**, shown as 1_1 on FIG. **6**, ensure that the entire beam **80** reflected from the portion of the entrance surface coated in reflective coating is incident on the portion of the beam splitting surface **56** that is not coated in beam splitting coating. Finally, the width of the first prism w_1, the height of the first prism h_1, the tilt angle π and the length of the beam splitting surface 1_1 ensure that the length of the optical paths taken by the first splat beam **72** and the second split beam **74** throughout the entire prism structure **50** are equivalent.

A closer examination of FIGS. **7** and **8** reveals that the second prism **62** is manufactured so that its shape ensures the following. Firstly, that the surface of the second prism adjacent to the beam splitting surface of the first prism **56** is matched to that surface. Secondly, that the width of the second prism, shown as w_2 on FIG. **7** and the angle of the second prism's reflective surface **64** relative to the entrance surface **54**, shown as θ on FIG. **7** ensure that the entire beam **80** reflected from the portion of the entrance surface coated in reflective coating is incident upon the second prism's reflective surface **64** and that the chief ray of the beam of light reflected from this surface **82** is perpendicular to the second prism's exit surface **84**. Thirdly, the width of the second prism w_2, the angle of the second prism's reflective surface relative to the entrance surface θ and the height of the surface of the second prism that is adjacent to the third

prism **86**, shown as h_2 on FIG. **7**, ensure that the entire beam reflected from the second prism's reflective surface **88** emerges from the exit surface of the second prism **84** and that none of second split beam **74** is incident on the second prism's reflective surface **64**. Fourthly, the angle between the surface of the second prism adjacent to the third prism **86** and the second prism's exit surface **84**, shown as ϕ in FIG. **7**, is as close to 90° as possible to prevent any total internal reflection that may result due to the tiny air gap between he two prisms. Finally, the width of the second prism w_2, the angle of the second prism's reflective surface relative to the entrance surface θ and the height of the surface of the second prism adjacent to the third prism h_2 ensure that the length of the optical paths taken by the first split beam **72** and the second split beam **74** throughout the entire prism structure **50** are equivalent.

A closer examination of FIG. **8** reveals that the third prism **66** is manufactured so that its shape ensures the following. Firstly, the surfaces of prisms two **62** and three **66** that are adjacent to each other **86** and **90** are matched to eliminate dispersion and aberration. Secondly, that its height, shown as h_3 on FIG. **8**, its width, shown as W_3 on FIG. **8** and the angle of its reflective surface **68** relative to the entrance surface **54**, shown as a on FIG. **8**, ensure that the chief ray of the beam of light reflected from the third prism's reflective surface **92** is perpendicular to the third prism's exit surface **94** and hat the entire beam of light reflected from the third prism's reflective surface **96** exits the third prism through the third prism's exit surface **94**. Finally, that the third prism's height h_3, width W_3 and the angle of its reflective surface relative to the entrance surface a ensure that the length of the optical paths taken by the first split beam **72** and the second split beam **74** throughout the entire prism structure **50** are equivalent. FIGS. **8A** and **8B** show the dimensions of a prism structure **50** manufactured to receive an F/4 input beam from a slit with a length of 12.8 mm. FIG. **8A** shows the dimensions of prism one **52** and FIG. **8B** shows the dimensions of prisms two and three **62,68**. An optical prescription for these prisms is contained in TABLES 1B–1D for an optical system presented In TABLE 2. The description of the tables is presented in the form utilized by the optical design program marketed under the tradename ZEMAX.

TABLE 1C-continued

Prism A Vertex Parameters			
Repeated Vertices			
Front	R 12340	Back	R 56780
Top	R 26730	Bottom	R 15840
Left side	R 12650	Right side	R 43780

TABLE 1D

Prism B Vertex Parameters					
Front Face Vertices			Back Face Vertices		
V1	−16	−10	0	V5	−16	−10	16
V2	−16	10.00357	3.53	V6	−16	1.27	16
V3	16	10.00357	3.53	V7	16	1.27	16
V4	16	−10	0	V8	16	−10	16
Repeated Vertices					
Front	R 12340	Back	R 56780
Top	R 26730	Bottom	R 15840
Left side	R 12650	Right side	R 43780

TABLE 1E

Prism C Vertex Parameters					
Front Face Vertices			Back Face Vertices		
V1	−16	−10	0	V5	−16	−10	25.15
V2	−16	10	0	V6	−16	10	5.15
V3	16	10	0	V7	16	10	5.15
V4	16	−10	0	V8	16	−10	25.15
Repeated Vertices					
Front	R 12340	Back	R 56780
Top	R 26730	Bottom	R 15840
Left side	R 12650	Right side	R 43780

A requirement in the manufacture of all the prisms, is that they must ensure the length of the optical paths taken by the first split beam **72** and the second split beam **74** through the

TABLE 1B

Non-Sequential Components Parameters							
Obj Type	Obj Name	Y Position	Z Position	Tilt X	Material	X ½ Width	Y ½ Width
Poly Obj	Prism A				KBr	Scale 1	Is Vol 1
Poly Obj	Prism B		5.851		KBr	Scale 1	Is Vol 1
Poly Obj	Prism C		21.851		KBr	Scale 1	Is Vol 1
Rectangle	A1 Mirror	4.15	—0.01	10	Mirror	16	5.85
Rectangle	A2 BmSp	−5.40	6.65	−45	mirror/KBr	16	4.64
Rectangle	C2 Mirror		37.0		Mirror	16	14

TABLE 1C

Prism A Vertex Parameters					
Front Face Vertices			Back Face Vertices		
V1	−16	−10	0	V5	−16	−10	5.85
V2	−16	10	0	V6	−16	10	9.38
V3	16	10	0	V7	16	10	9.38
V4	16	−10	0	V8	16	−10	5.85

prism structure **50** are equivalent. This requirement means that each of the rays in the split beams of light **72,74** must travel the same distance in each of the materials present in the prism structure **50** as the corresponding ray in the other split beam of light. A closer examination of FIGS. **9, 10** and **11** demonstrates that the prism structure **50** ensures that this occurs. In each of these figures the optical distance of the ray of the first split beam of light is the sum of the three distances d_1, d_2 and d_3 and the optical distance traveled by the corresponding ray of the second split beam of light is the sum of the two distances d_4 and d_5. In each of FIGS. **9, 10** and **11**, $d_1+d_2+d_3=d_4+d_5$. Minor variations in the width of

the air gaps between prisms one and two and prisms two and three are inconsequential. The optical path length for the prism structure shown in FIGS. 8A and 8B is 47 mm and the width of the air gaps is approximately 10 microns. This difference is unimportant because it does not have a signifi- cant effect on the marginal ray angles of the two split beams **72,74**, when they are incident on the Fourier optical system **16**.

A variation on the embodiment of the beam shearing system **14'** described above is shown in FIG. **11A**, this arrangement replaces the prism structure **50** with an struc- ture involving parallel plates acting as a beam splitter **150** and three mirrors **152**, **154** and **156**. The basic arrangement of **3** reflections for the first split beam **72'** and one reflection for the second split beam **74'** is maintained. Use of this beam shearing system **14'** places a limitation on the F/# of the input beam and the possible size of the separation between the two emerging beams **30'** and **32'**, shown as Δs on FIG. **11A** because the beams diverge more rapidly in air than in a higher index material.

A closer examination of FIG. **11A** reveals that the static interferometer must be manufactured in the following way. The entrance slit **26'** must be mounted inside the first mirror **152** and the parallel plate beam splitter **150** oriented per- pendicular to the chief ray of the entrance beam **158**. The parallel plate beam splitter is coated on the second surface of the first parallel plate, and the second parallel plate is of equal thickness to the first plate to ensure that the total optical path length traveled by both beams is equal.

The first mirror is tilted at an angle that ensures that the first split beam **72'** is reflected from the beam splitter **150** to the second mirror **154**. The slit must be small compared to the returning beam **72'** to minimize the amount of light lost. The second and third mirrors are aligned so that the chief rays of the two emerging beams **30'** and **32'** are parallel. Overall, the mirrors must be arranged to ensure that both split beams of light **72',74'** travel the same optical distance.

Another variation of the beam shearing system is shown as **14"** in FIG. **11B** This variation is designed for use with a collimated input beam. It uses a similar parallel plate and mirror configuration as in FIG. **11A** except that the beam splitter **150'** is tilted with respect to the input beam **70'**. The beam splitter **150'** splits the input beam into two beams **72"**

and **74"**. These beams are then reflected in a similar fashion to the beam shearing system shown as **14'** in FIG. **11A**. However, because the beams are collimated, the beam shearing system **14"** is able to recombine the two split beams at an exit pupil plane without the need for the Fourier optical system. The beam shearing system places a limitation on the F/# of the fore-optics to ensure that the exit pupil is sufficiently far from the fore-optics to enable the configu- ration shown.

The best performance of the static interferometer **10** is achieved, when the fore-optics are as shown in FIG. **12**. Manufacturing the fore-optics in this way ensures that the pupil of the fore-optics is shifted to one side of the optical axis. This results in the chief ray of the input beam **22** striking the exit pupil **34** at the edge of the detector array **18**, enabling a single sided interferogram to be recorded. Using a single sided interferogram instead of a complete interfero- gram reduces the size of the other components of the static interferometer **10** by a factor of two, without losing any information or signal.

Examining the illustration in FIG. **12** in greater detail, reveals that the fore-optics **12** comprise a scan mirror **160** and three coaxial aspheric mirrors **162**, **164** and **166**. The first coaxial aspheric mirror **162** is an even asphere and the other two mirrors are simple conics **164**, **166**. The input beam **22** is reflected by the scan mirror onto the first coaxial asphere **162**, which reflects the light onto the second coaxial asphere **164**. The light is finally reflected by the third coaxial asphere **166**, which focuses the light onto the entrance slit **26**. The focused beam **168** is telecentric and it is observed that its chief ray strikes one side of the aperture stop **170** of the second coaxial aspheric mirror because the pupil of the fore-optics is shifted. The four mirrors **160**, **162**, **164**, **166** are co-axial, which means that the fore-optics are simple to construct.

A specific example of the mirror configuration of the fore-optics **12**, illustrated in FIG. **12**, is provided in part of TABLE 2. The description of TABLE 2 is presented in the form utilized by the optical design program marketed under the tradename ZEMAX. The prescription in TABLE 2 assumes that the output light **24** is F/4 in the tangential y-plane and F/5 in the sagiital X-plane.

TABLE 2

	ZEMAX PRESCRIPTION: Telescope and Prism in 1.2 cm⁻¹ Imaging Spectrometer.							
Surface	Type	Name	Radius Mm	Thickness mm	Conic	Coeff on r4	Coeff on r6	Coeff on r8
Object			Infinity	infinity				
1	apert	ent port		130				
2	coord	tilt Y				6°		
3	mirror	Scan	Infinity	−140				
4	coord	tilt Y				6°		
5	mirror	TM1 asph	631.6257	122.6101	−3.2	−8.326e-10	3.06657e-14	−2.45337e-18
STOP	mirror	TM2 conic	176.0148	−122.6101	0.155589			
7	mirror	TM3 conic	244.9272	215.1279	0.182058			
8	coord	Decenter Y				31.2483 mm		
9	apert	Slit		3				
10	coord	Decenter Y				3.2 mm		
11	NSC	Prism			Reverse rays: 1	exit location Y: −10.001 mm	exit location Z: 16.1112 mm	exit tilt X: −90°
12	standrd	Gap		−0.042				
13	coord	Decenter Y				−12 mm		
14	coord	tilt Y		−134.468		−13.383°		
15	coord	Decenter X				13.927 mm		

TABLE 2-continued

ZEMAX PRESCRIPTION: Telescope and Prism in
1.2 cm^{-1} Imaging Spectrometer.

Surface	Type	Name	Radius Mm	Thickness mm	Conic	Coeff on r4	Coeff on r6	Coeff on r8
16	mirror	X toroid FM1	136.1947 148.5778	113.6148		−9.0040886e-9	−2.775225e-13	
17	mirror	X toroid FM2	−74.663 99.7735	−77.3079		5.3235734e-6	−2.8462433e-7	−8.10146e-10
18	mirror	asphere FM3	171.811	77.3079		−9.2187783e-8	1.719915e-11	−2.72977e-15
19	mirror	Y toroid FM4	−298.0 −209.474	−132.6079		7.7831648e-8	−1.816862e-11	
20	coord	tilt Y			14.582°			
Image		focal plane	infinity					

NOTE 1:
Spectral resolution is 1.21 cm^{-1}. Pupil width is 50 mm, X-Field is +/− 1.888°, Y-Field is 9°, and wavelength is 13 μm. Design is valid between 5 and 20 μm with KBr or 5 and 50 μm with CsI. Tangential width of stop is 30.6 mm; sagittal width is 24.6 mm. Stop is shifted along tangential plane away from slit so that chief ray is 6.2 mm from short side and 23.8 mm from long side of stop. Detector is 12.8 × 16 mm.
NOTE 2:
In Zemax the X toroids are generated by placing coordinate breaks of 90° and −90° before and after a standard "Y" toroid. However, many optical design packages explicitly call out Y and X toroids to omit the two coordinate breaks. Therefore the coordinate breaks for the X toroids have been omitted in the above prescription. The top number is the radius, and the bottom number is the radius of rotation.
NOTE 3:
Decenters, tilts, and NSC parameters are listed in the columns with the headings "Conic", "Coeff. on r4", "Coeff. on r6", and "Coeff. on r8".

The best performance of the static interferometer **10** is achieved, when the two beams emerging from the beam shearing system **30,32** are recombined using the Fourier optical system **16** shown in FIGS. **13** and **14**. The Fourier optical system **16** is manufactured to maximize the image focal length and spatial resolution of the Fourier optical system by ensuring that the imaging and collimating functions are performed by the same optical components. It is also telecentric in the tangential plane to ensure spectral radiometric purity.

Examining the illustration in FIGS. **13** and **14** in greater detail, it shows a form of the Fourier optical system **6** having four mirrors and which is completely anamorphic. The first and second mirrors **180,182** are aspheric toroids that each have an aspherical surface in the X plane and a spherical surface in the Y plane. The third mirror **184** is an even asphere and the fourth mirror **186** is an aspheric toriod with an aspherical surface in the Y plane and a spherical surface in the X plane. All four mirrors are co-axial, with a vertices along the common axis **190**. This property ensures that no alignment of the mirrors of the Fourier optical system is required. Their mounting (not shown) is a simple 'bolt and go' configuration.

The mirrors are manufactured to ensure that the two beams emerging from the beam shearing system **30,32** strike the first mirror **180** and are reflected onto he second mirror **182**, which is located inside a cut out of the fourth mirror **186**. The mirrors also ensure that the two beams are then reflected onto the third mirror **184** and from there onto the fourth mirror **186**. The combination of the four mirrors ensures that the light reflected from the fourth mirror **186** forms two collimated exit beams **192** and **194** that exit the Fourier, optical system through a cut-out of the third mirror **184**. The manufacture of the mirrors ensures that the two exit beams **192,194** combine and form a pupil plane **34** in the Y plane and an image plane **36** in the X plane, with both planes located at the same point along the optical axis **190**.

A specific example of the mirror configuration of he Fourier optical system **16**, illustrated in FIGS. **13** and **14**, is also provided in TABLE 4. The description of TABLE 3 is presented in the form utilized by the optical design program marketed under the tradename ZEMAX. Manufacturing the Fourier optical system **16** according to the prescription in TABLE 4 results in it having focal length in the X and Y plane of 64 mm.

Manufacturing the fore-optics **12**, the beam shearing system **14** and the Fourier optical system **16** according to the prescriptions contained in TABLES 1B–1E and 2, results in the static interferometer achieving a spectral resolution of 1.2 cm^{-1} over the spectral bandpass of the material used to construct the prism structure **50**. If the length of the entrance slit **26** is chosen to be 12.8 mm, then the static interferometer **10** will have a 3.8° field of view (FOV).

An alternative method of manufacturing the Fourier optical system **16'** to achieve a broadband, high spectral resolution, off-axis point spectrometer is shown in FIG. **15**. It consists of four off-axis aspheres, **180'**, **182'**, **184'** and **186'**, which generate two very high quality collimated beams. These beams generate a 0.5 cm^{-1}, single-sided interferogram across a 25 mm detector array.

FIG. **16** shows a variation on this alternative method of manufacturing the Fourier optical system **16"**. This variation uses the same four off-axis aspheres, **180"**, **182"**, **184"** and **186"**, but uses a fold mirror **200** and a cylindrical mirror **202** to compress the collimated beam to 1 mm in the X direction to improve the signal efficiency and reduce the width of the detector array **18**. A cylindrical mirror **202** is preferable to a refractive cylindrical lens because the rays of the collimated beams passing through the thicker part of a lens would be shifted in the Y direction with respect to the rays passing through the thinner part of that lens. An optical prescription for this Fourier optical system **16"** is contained in TABLE 2.

TABLE 3

ZEMAX PRESCRIPTION: 0.5 cm⁻¹ Point Spectrometer

Surface	Type	Name	Radius mm	Thickness mm	Coeff on r4		Coeff on r6
Object			infinity	infinity			
STOP	stanrd	ent pupil		100			
2	paraxial	telescope	100	100			
3	apert	slit		3			
4	KBr	prism		93			
5	coord	tilt X			−45°		
6	mirror	C2					
7	coord	tilt X		−15	−45°		
8	standrd	prism exit					
9	coord	decenter Y			−27.75	mm	
10	coord	tilt Y		−138.7318	−4.6515°		
11	coord	decenter X			±13.5551	mm	
12	mirror	M1 asphere	146.0153	83.9595	1.5855e-9		−4.1844e-14
13	mirror	M2 asphere	109.167	−95.2057	4.1951e-7		−8.3999e-10
14	mirror	M3 asphere	235.8198	95.2057	4.1801e-8		−1.0609e-13
15	mirror	M4 asphere	−295	−120.4057	4.3190e-8		2.7327e-12
16	coord	dec X tilt Y			12.1	mm	4.6515°
17	coord	tilt Y			20°		
18	mirror	fold mirror					
19	coord	tilt Y		26.12	20°		
20	coord				−20°		
21	mirror	X toroid	−56				
22	coord			−26	−20°		
Image		focal plane	infinity				

NOTE 1:
Spectrometer can achieve 0.5 cm⁻¹. Pupil width is 50 mm, X,Y-Fields are +/− 0.55° and wavelength is 13 μm. Design is valid between 5 and 20 μm with KBr or 5 and 50 μm with CsI. Tangential width of stop is 25 mm; sagittal width is 12.5 mm. Stop is shifted along tangential plane by −9.3 mm. A paraxial lens is used to simulate the telescope. Shifts in the ± X direction simulate the prism. Cylindrical mirror compresses beam without adversely affecting interferogram. Detector array is 1 × 25 mm
NOTE 2:
Decenters and tilts are listed in the column with the heading "Coeff. on r4".

An alternative method of manufacturing the Fourier optical system 16‴ to achieve a large FOV, on-axis refractive imaging spectrometer is shown in FIGS. 17 and 18. This configuration is appropriate where the spectral bandwidth requirements are not too broad. The imaging focal length can be made significantly shorter than the interferogram focal length of the Fourier optical system 16‴ to increase the FOV. The design, shown in FIGS. 17 and 18, uses three aspheric Ge lenses 210, 212 and 214 to collimate the beams emerging from the beam shearing system 30,32 to form a pupil plane 34 in one axis and to form an image plane 36 in the other axis. An optical prescription for this Fourier optical system 16‴ is contained in TABLE 4.

TABLE 4

ZEMAX PRESCRIPTION: 1.2 cm⁻¹ On-Axis Imaging Spectrometer

Surface	Type	Name	Radius mm	Thickness mm	Coeff on r4	Coeff on r6	Coeff on r8
Object			infinity	infinity			
STOP	standrd	ent pupil		64			
2	paraxial	Telescope	64	64			
3	apert	Slit		3			
4	KBr	Prism		40.158			
5	coord	tilt X			−45°		
6	mirror	C2					
7	coord	tilt X		−6.842	−45°		
8	standrd	prism exit		21.2106			
9	Ge	L1 asphere	292.1871	3	−3.1404e-7	−4.477e-11	4.1884e-13
10	—	Y toroid	−285.5098	14.5723			
11	Ge	L2 standard	67.2090	2.35			
12	—	asphere	−60.0	38	−1.0316e-7	1.76843e-11	−3.6181e-11
18	Ge	L3 window	infinity	1.5			
21		Y toroid	−63.6822	15	−1.1044e-5	1.78802e-7	
Image		focal plane	infinity				
Object			infinity	infinity			
STOP	standrd	ent pupil		64			
2	paraxial	telescope	64	64			
3	apert	slit		3			
4	KBr	prism		40.158			

TABLE 4-continued

			ZEMAX PRESCRIPTION: 1.2 cm⁻¹ On-Axis Imaging Spectrometer				
Surface	Type	Name	Radius mm	Thickness mm	Coeff on r4	Coeff on r6	Coeff on r8
5	coord	tilt X			45°		
6	mirror	C2					
7	coord	tilt X		−6.842	45°		
8	standrd	prism exit		21.2106			
9	Ge	L1 asphere	292.1871	3	−3.1404e-7	−4.477e-11	−4.1884e-13
10	—	Y toroid	−285.5098	14.5723			
11	Ge	L2 standard	67.2090	2.35			
12	—	asphere	−60.0	38	−1.0316e-7	1.76843e-11	−3.6181e-11
18	Ge	L3 window	infinity	1.5			
21		Y toroid	−63.6822	15	−1.1044e-5	1.78802e-7	
Image		focal plane	infinity				

NOTE 1:
Pupil width is 16 mm, Y-Fields are +/−12° and wavelength is 13 μm. Design is valid between 5 and 16 μm. Width of stop in X direction is 16 mm. Width in Y direction is 12.8 mm. Stop can be shifted along tangential plane to generate single-sided interferogram and achieve 1.2 cm⁻¹ spectral resolution. A paraxial lens is used to simulate the telescope. Coordinate break shifts in ± X simulate the prism. Detector array is 12.8 × 16 mm.
NOTE 2:
In this design the pupil plane is in the X direction and the image plane is in the Y direction. This enabled "Y" toroids to be used to generate the image, and "Y" toroids do not require coordinate brakes to rotate them about the Z axis.
NOTE 3:
Tilts are listed in the column with the heading "Coeff. on r4".

Closer inspection of FIG. 2 illustrates that a 2 dimensional detector array is located at the pupil 34 and image 36 planes. This array makes measurements of light intensity in both the pupil and image planes. Large format AlGaAs Quantum Well Infrared Photoconductor (QWIP) arrays are the most appropriate detectors because their pixel to pixel responsivity is uniform. AlGaAs QWIP arrays can be fabricated with an operability greater than 99.99%, an uncalibrated uniformity better than 2% and a calibrated uniformity better than 0.3%. They can also be thermally cycled indefinitely, are radiation hard and remain stable after calibration.

AlGaAs QWIP detector arrays are not the only type of detector that can be used. Other examples of detector arrays that could be utilized by the static interferometer 10 include InSb, HgCdTe, microbolometers, thermopiles, CCDs and active pixel sensor (APS) arrays.

The processor unit 20 analyzes the data recorded by the detector array 18. This unit digitizes the data, stores it, can analyze it in a number of ways, including the two following methods and can output any results. The data recorded by the detector array 18 corresponds to a series of interferograms. The first possible method of analyzing this data is to perform a digital fast fourier transform (FFT) to convert each interferogram into a spectrum, which can then be further analyzed. An example would be where the spectrum s analyzed to determine the overall chemical composition of the scene being viewed.

An alternative method of analyzing the data is to use the interferograms as matched filters to detect distinct features within the interferograms. An example of this would be to detect the presence of a single chemical in the scene being viewed. This process involves using a filter shape that indicates the presence or absence of hat feature, when the filter is convolved with the interferogram. An advantage of using this second technique is that it is less computationally intensive than performing numerous FFTs. Another advantage is that the interferogram automatically separates broadband features, such as emissions from a planet's surface from narrowband features, such as are created by constituent gases in the planet's atmosphere.

At shorter wavelengths it may be necessary to use heterodyning at the detector array. Heterodyning is appropriate if a full cycle of the interferogram 220 of FIG. 19 is located inside one pixel 222 of the detector array 18. When this occurs, the constructive 224 and destructive 226 half cycles of the interferogram will cancel each other out and the detector 18 will detect zero light intensity for that pixel 222. This phenomenon can be avoided by using a blocking filter 228. This filter discards the destructive portion of the interferogram 226, ensuring that only the constructive portion of the interferogram 224 is incident on the pixel of the detector array 222. In a broadband system, the blocking filter must be manufactured so that its pattern has a frequency that is equal to or lower than the lowest frequency in the predetermined spectral passband. The detector will then detect that light to be frequency zero and light with higher frequency will be detected as having a frequency equal to the actual frequency of the detected radiation minus the frequency of the radiation of lowest frequency. interferogram 220, using a detector 18 that would not have enough pixels to measure the intensity of the interferogram without the use of a blocking filter.

While the preferred embodiment has been described and illustrated, various substitutions and modifications may be made thereto without departing from the scope of the invention. Accordingly, it is to be understood that the present invention has been described by way of illustration and not limitation.

I claim:

1. A spectral resolving system comprising:

an entrance slit structure having an entrance slit extending in a first direction for receiving a beam of light having a photon flux within a predetermined spectral pass band;

a beam shearing system including:

a beam splitter on the surface of a prism that is aligned at an angle to the first direction so that the received beam of light is split into two separate beams;

an air gap adjacent the surface of the prism on which the beam splitter is located;

a reflective subsystem having a plurality of reflective surfaces defining separate light paths of equal optical path length for the two separate beams, the reflective

surfaces arranged such that when the two beams
emerge from the beam shearing system they contain
more than 50 percent of the photon flux and the chief
rays of the two separate beams are substantially
parallel to each other; and

wherein the angle at which the beam splitter is aligned
is less than the critical angle above which total
internal reflection of a portion of the beam of light
occurs; and

an optical system configured to recombine the two sepa-
rate beams of light emerging from the beam shearing
system onto an exit pupil.

2. The spectral resolving system of claim **1** wherein the
optical system is also configured to recombine the separate
beams of light emerging from the beam shearing system to
create an image substantially perpendicular to the exit pupil
plane.

3. The spectral resolving system of claim **2** wherein:

the optical system has an optical axis;

the exit pupil is located in one of the group consisting of
a tangential plane and a sagittal plane relative to the
beam shearing system;

the image is located in the other of the group consisting
of a tangential plane and a sagittal plane relative to the
beam shearing system; and

the exit pupil and the image are located at substantially the
same position along the optical axis.

4. The spectral resolving system of claim **1** wherein the
optical system is telecentric in object space, where the object
of the optical system is the entrance slit.

5. The spectral resolving system of claim **1** wherein the
optical system is anamorphic.

6. The spectral resolving system of claim **1** wherein the
optical system cancels aberrations when it recombines the
two beams of light that emerge from the beam shearing
system.

7. A static interferometer comprising:

fore-optics having a chief ray and a pupil that is asym-
metric relative to the chief ray and configured to collect
light and focus it into a beam;

a spectral resolving system comprising:

an entrance slit structure having an entrance slit extend-
ing in a first direction for receiving a beam of light;

a beam shearing system including:

a beam splitter aligned at an angle to the first
direction configured to split the received beam of
light into two separate beams;

a reflective subsystem having a plurality of reflective
surfaces defining separate light paths of equal
optical path length for the two separate beams, the
reflective surfaces arranged such that when the
two beams emerge the chiefrays of the two sepa-
rate beams are substantially parallel to each other;
and

an optical system configured to recombine the two
separate beams of light emerging from the beam
shearing system onto an exit pupil.

8. A static interferometer comprising:

fore-optics having a chief ray and a pupil that is asym-
metric relative to the chief ray and configured to collect
light and focus it into a beam;

a spectral resolving system comprising:

an entrance slit structure having an entrance slit extend-
ing in a first direction for receiving a beam of light;

a beam shearing system including:

a beam splitter aligned at an angle to the first direction
configured to split the received beam of light into
two separate beams;

a reflective subsystem having a plurality of reflective
surfaces defining separate light paths of equal optical
path length for the two separate beams, the reflective
surfaces arranged such that when the two beams
emerge the chief rays of the two separate beams are
substantially parallel to each other; and

an optical system configured to recombine the two
separate beams of light emerging from the beam
shearing system onto an exit pupil; and

a detector located at the exit pupil.

9. The static interferometer in claim **8** wherein the detec-
tor is configured to record pixels of incident radiation
intensity.

10. The static interferometer in claim **9** further compris-
ing:

a data processing system connected to the detector; and

wherein the data processing system performs Fast Fourier
Transforms on the digitized measurements to obtain the
spectral composition of the incident radiation.

11. The static interferometer in claim **9** further compris-
ing:

a data processing system connected to the detector; and

wherein the data processing system convolves the mea-
surements with filters to detect the, presence or absence
in the spectrum of the incident radiation of frequencies
of radiation characteristically emitted or absorbed by
particular substances.

12. The static interferometer in claim **8**, wherein the two
beams of light arc recombined to form a single sided
interferogram at the exit pupil.

13. The static interferometer in claim **12** wherein the
reflective surfaces of the reflective subsystem are configured
such that when the two beams emerge from the beam
shearing system they contain more than 50 percent of the
photon flux of the received beam of light.

14. The static interferometer in claim **8**, wherein the chief
ray of light collected by the fore-optics is substantially to
one side of the optical axis of the beam formed by the
fore-optics.

15. The static interferometer in claim **8**, wherein the
fore-optics are telecentric.

16. The static interferometer of claim **8**, wherein the
optical system also focuses the separate beams of light
emerging from the beam shearing system to create an image.

17. The static interferometer of claim **16** wherein:

the optical system has an optical axis;

the exit pupil is located in one of the group consisting of
a tangential plane and a sagittal plane relative to the
beam shearing system;

the image is located in the other of the group consisting
of a tangential plane and a sagittal plane relative to the
beam shearing system; and

the exit pupil and the image are located at substantially the
same position along the optical axis.

18. The static interferometer of claim **8**, wherein the
fore-optics have an asymmetric pupil and are telecentric in
image space.

19. A beam shearing system comprising:

an entrance slit structure having an entrance slit extending
in a first direction for receiving a beam of light having
a photon flux within a predetermined spectral pass
band;

a beam splitter aligned at an angle to the first direction so
that the received beam of light is split into two separate
beams;

a reflective subsystem having a plurality of reflective
surfaces defining separate light paths of equal optical

path length for the two separate beams, the reflective surfaces arranged such that one of the separate beams undergoes one reflection and the other of the separate beams undergoes three reflections and that when the two beams emerge from the beam shearing system they contain more than 50 percent of the said photon flux.

20. The beam shearing system of claim 19, wherein an air gap exists between the beam splitter and one of the bodies.

21. The static interferometer of claim 20, wherein the fore-optics are constructed using a single lens, two or more lenses, a configuration of mirrors or catadioptric systems.

22. The beam shearing system in claim 19 wherein the two beams emerging from the beam shearing system contain substantially all of the light entering the system through the entrance sit.

23. The beam shearing system in claim 19 wherein the two light paths defined by the reflective subsystem cause the wave fronts of the two separate beams to remain substantially in phase relative to one another when the beams emerge from the beam shearing system.

24. The beam shearing in claim 19 wherein the plurality of reflective surfaces are further arranged so that the separate beams of light are of substantially equal intensity, when they emerge from the beam shearing system.

25. The beam shearing system in claim 19 wherein:

the reflective subsystem comprises a plurality of bodies with a beam splitter therebetween; and

the entrance and exit surfaces of the plurality of bodies arc substantially perpendicular to the chief ray of the received beam of light.

26. A static interferometer comprising:

fore-optics for collecting light and collimating into a beam, the fore-optics possessing an exit pupil;

a beam shearing system comprising:

an entrance slit structure having an entrance slit extending in a first direction for receiving a beam of light having a photon flux within a predetermined spectral pass band;

a beam shearing system comprising:

a beam splitter aligned at an angle to the first direction so that the received beam of light is split into two separate beams;

a reflective subsystem having a plurality of reflective surfaces defining separate light paths of equal optical path length for the two separate beams, the reflective surfaces arranged such that one of the separate beams undergoes one reflection and the other of the separate beams undergoes three reflections and that when the two beams emerge from the beam shearing system they contain more than 50 percent of the said photon flux; and

a detector located at said exit pupil where the two beams emerging from the beam shearing system converge.

27. The static interferometer in claim 26 wherein the detector comprises a detector array, read out electronics and a data processing system.

28. The static interferometer in claim 27 wherein:

the detector array records the intensity of the radiation incident on its pixels;

the read out electronics digitizes the intensity measurements made by the detector array and transfers them to the data processing system; and

the data processing system manipulates the digitized measurements to obtain information about the spectrum of the incident radiation.

29. The static interferometer in claim 28 wherein the data processing system performs Fast Fourier Transforms on the digitized measurements to obtain the spectral composition of the incident radiation.

30. The static interferometer in claim 29 wherein the data processing system convolves the digitized measurements with digital filters to detect the presence or absence in the spectrum of the incident radiation of frequencies of radiation characteristically emitted or absorbed by particular substances.

31. The static interferometer in claim 26 which further comprises:

an anamorphic optical'system possessing an optical axis;

the exit pupil being perpendicular to the optical axis;

the optical system focusing the two beams emerging from the beam shearing system to create an image; and

the image being perpendicular to the exit pupil and perpendicular to the optical axis.

32. A beam shearing system for shearing an incident beam of light having a chief ray, comprising:

a first prism possessing a surface acting as a beam splitter;

a second prism positioned to create an air gap between the second prism and the surface;

wherein the first and second prisms are positioned such that the incident beam of light is incident on the surface at an angle that substantially prevents total internal reflection;

wherein the incident beam of light is split by the beam splitter into two separate beams of light that emerge from the beam shearing system; and

wherein the two beams of light are substantially parallel when they emerge from the beam shearing system and contain more than 50% of the incident light.

33. A beam shearing system for shearing an incident beam of light having a chief ray, comprising:

a first prism possessing a surface acting as a beam splitter;

a second Prism positioned to create an air gap between the second prism and the surface;

wherein the first and second prisms are positioned such that the incident beam of light is incident on the surface at an angle that substantially prevents total internal reflection;

wherein the incident beam of light is split by the beam splitter into two separate beams of light that emerge from the beam shearing system; and

wherein the two beams of light are substantially parallel when they emerge from the beam shearing system and contain more than 50% of the incident light; and

wherein both the beams of light emerging from the beam shearing system include infrared radiation.

34. A beam shearing system for shearing an incident beam of light having a chief ray, comprising:

a first prism possessing a surface acting as a beam splitter;

a second prism positioned to create an air Rap between the second prism and the surface;

wherein the first and second prisms are positioned such that the incident beam of light is incident on the surface at an angle that substantially prevents total internal reflection;

wherein the incident beam of light is split by the beam splitter into two separate beams of light that emerge from the beam shearing system; and

wherein the two beams of light are substantially parallel when they emerge from the beam shearing system and contain more than 50% of the incident light; and

wherein both the beams of light emerging from the beam shearing system include ultraviolet radiation.

* * * * *